JOINT WMO TECHNICAL PROGRESS REPORT ON THE GLOBAL DATA PROCESSING AND FORECASTING SYSTEM AND NUMERICAL WEATHER PREDICTION RESEARCH ACTIVITIES FOR 2019

Japan Meteorological Agency

1. Summary of highlights

(1) Hybrid four-dimensional variational data assimilation involving the use of a Local Ensemble Transform Kalman Filter was employed and an incremental method with outer-loop iterations was adopted in atmospheric analysis for the Global Spectral Model in December 2019. (4.2.1.1 (1))

(2) Operational use of NOAA-20 ATMS and CrIS Radiance Data in JMA's Global NWP system was implemented on 5 March 2019. (4.2.1.2 (1))

(3) Operational use of GOES-16 clear-sky radiance data in JMA's global NWP system was implemented on June 18 2019. (4.2.1.2 (2))

(4) All-sky microwave radiance assimilation into JMA's global NWP system was implemented in December 2019. (4.2.1.2 (3))

(5) Operational use of Metop-C ASCAT wind data in JMA's global NWP system was implemented on December 11 2019. (4.2.1.2 (4))

(6) Operational use of surface-sensitive clear-sky radiance data in JMA's mesoscale NWP system was implemented on March 26 2019. (4.3.1.2 (1))

(7) Bias correction of aircraft temperature data in JMA's mesoscale NWP system was implemented on March 26 2019. (4.3.1.2 (2))

(8) Enhanced use of ground-based GNSS data in JMA's mesoscale NWP system was implemented on March 26 2019. (4.3.1.2 (3))

(9) Operational use of ocean vector wind (OVW) data from ASCAT 12.5 km coastal wind data in JMA's mesoscale NWP system was implemented on March 26 2019. (4.3.1.2 (4))

(10) The Meso-Scale Model forecast range for the initial times of 00 and 12 UTC was extended to 51 hours in March 2019. (4.3.2.1 (1))

(11) The Local Forecast Model forecast range for all initial times was extended to 10 hours in March 2019. (4.3.2.1 (2))

(12) Operation of the Meso-scale Ensemble Prediction System (MEPS) was implemented in June 2019. (4.3.5.1)

(13) Snow Depth and Snowfall Amount Analysis were introduced in November 2019. (4.4)

(14) High-resolution sea surface temperature analysis for the western North Pacific was implemented in the Meso-Scale Model and the Local Forecast Model in March 2019. (4.5.1.1 (2))

2. Equipment in use

On 5 June 2018, an upgraded version of the computer system used for numerical analysis/prediction and satellite data processing was installed at the Office of Computer Systems Operations in Kiyose (around 30 km northwest of JMA's Tokyo Headquarters) and at the Osaka Regional Headquarters. The Kiyose, Tokyo and Osaka locations are connected via a wide-area network. The computer types used in the system are listed in Table 2-1, and further details are provided in JMA (2019).

Table 2-1 System computer types

Supercomputers (Kiyose)	Cray XC50
Subsystems	2
Nodes per subsystem	2,816 computational 40 I/O
Processors	2 sockets for Intel Xeon Platinum 8160 processors per computational node 1 Intel Xeon E5-2699v4 processor per I/O node
Performance	9.08 PFlops per subsystem (3225.6 GFLOPS per node)
Main memory	264 TiB per subsystem (96 GiB per node)
High-speed storage*	DDN ExaScaler Lustre file system (4.8 PiB per subsystem)
Data transfer rate	14 GB/s (one way) (between any two nodes)
Operating system	Cray Linux Environment 6.0/SUSE 12.2

* Dedicated storage for supercomputers

Satellite Data Reception Servers (Kiyose) Server:	HPE ProLiant DL360 Gen9
Servers	5
Processors	2 sockets for Intel Xeon E5-2620v3 processors
Main memory	64 GiB per server
Operating system	Red Hat Enterprise Linux Server 7.3

Satellite Imagery Processing Producing Servers (Kiyose):	HPE ProLiant DL580 Gen9
Servers	8
Processors	4 sockets for Intel Xeon E7-8880v3 processors
Main memory	256 GiB per server
Operating system	Red Hat Enterprise Linux Server 7.3

Satellite Product Servers (Kiyose):	HPE ProLiant DL380 Gen9
Servers	10
Processors	2 sockets for Intel Xeon E5-2670v3 processors
Main memory	192 GiB per server

Operating system	Red Hat Enterprise Linux Server 7.3

Operation Control Servers (Kiyose): Hitachi HA8000 RS210AN1

Servers	8
Processors	2 sockets for Intel Xeon E5-2640v3 processors
Main memory	32 GiB per server
Operating system	Red Hat Enterprise Linux Server 7.3

Division Task Processing Servers (Kiyose): HPE ProLiant DL580 Gen9

Servers	12
Processors	4 sockets for Intel Xeon E7-8880v3 processors
Main memory	128 GiB per server
Operating system	Red Hat Enterprise Linux Server 7.3

Decoding Servers (Kiyose): HPE ProLiant DL580 Gen9

Servers	2
Processors	4 sockets for Intel Xeon E7-8860v3 processors
Main memory	256 GiB per server
Operating system	Red Hat Enterprise Linux Server 7.3

NWP BCP Servers (Osaka): HPE ProLiant DL360 Gen9

Servers	2
Processors	2 sockets for Intel Xeon E5-2680v3 processors
Main memory	256 GiB per server
Operating system	Red Hat Enterprise Linux Server 7.3

Satellite Data Reception Servers (Osaka): HPE ProLiant DL360 Gen9

Servers	2
Processors	2 sockets for Intel Xeon E5-2620v3 processors
Main memory	64 GiB per server
Operating system	Red Hat Enterprise Linux Server 7.3

Satellite Imagery Processing Servers (Osaka): HPE ProLiant DL360 Gen9

Servers	4
Processors	2 sockets for Intel Xeon E5-2698v3 processors
Main memory	128 GiB per server
Operating system	Red Hat Enterprise Linux Server 7.3

External Storage System (Kiyose)

Shared storage**	Hitachi VSP G800 (6.06 PB total, RAID 6)

High-capacity storage (1) **	Hitachi VSP G800 (6.08 PB total, RAID 6)
High-capacity storage (2) **	Hitachi VSP G800 (3.04 PB total, RAID 6)
High-capacity storage (3) **	Hitachi VSP G800 (16.02 PB total, RAID 6)
Long-term Archival Storage	IBM TS4500 tape library (80 PB total)

** Shared by supercomputers and servers

Wide Area Network

Between HQ and Kiyose: Network bandwidth 1,200 Mbps (two independent 100-Mbps and 1-Gbps (best-effort) WANs)

Between Kiyose and Osaka: Network bandwidth 200 Mbps (two independent 100-Mbps WANs)

3. Data and Products from GTS and other sources in use

3.1 Observation

A summary of data received through the GTS and other sources and processed at JMA is given in Table 3-1.

Table 3-1 Number of observation reports in use

SYNOP/SHIP/SYNOP MOBIL	200,000/day
BUOY	58,000/day
TEMP/PILOT	7500/day
AIREP/AMDAR	1,100,000/day
PROFILER	8,000/day
AMSR2	14,000,000/day
GPM/GMI	10,200,000/day
Coriolis/WindSat	6,800,000/day
FY-3/MWRI	12,000,000/day
Aqua/AIRS, AMSU-A	270,000/day
NOAA/AMSU-A	960,000/day
Metop/AMSU-A	640,000/day
NOAA/MHS	5,800,000/day
Metop/MHS	5,800,000/day
Metop/IASI	600,000/day
Metop/ASCAT	8,000,000/day
Suomi-NPP/ATMS	3,000,000/day
Suomi-NPP/CrIS	3,000,000/day
NOAA/ATMS	3,000,000/day
NOAA/CrIS	3,000,000/day
Megha-Tropiques/SAPHIR	9,000,000/day
GOES/CSR	6,200,000/day
Himawari/CSR	1,300,000/day
METEOSAT/CSR	1,800,000/day
GNSS-RO	460,000/day
AMV	10,000,000/day
SSMIS	14,000,000/day
GNSS-PWV	4,200,000/day
AMeDAS	232,400/day

Radar Reflectivity	4,200/day
Radial Velocity	4,200/day

3.2 Forecast products

Grid Point Value (GPV) products of the global prediction model from ECMWF, NCEP, UKMO, BOM, ECCC, DWD, KMA and CMA are used for internal reference and monitoring. The products of ECMWF are received via the GTS, and the other products are received via the Internet.

4. Forecasting systems

4.1 System run schedule and forecast ranges

Table 4.1-1 summarizes the system run schedule and forecast ranges.

Table 4.1-1 Schedule of the analysis and forecast system

Model	Initial time (UTC)	Run schedule (UTC)	Forecast range (hours)
Global Analysis/Forecast	00	0220 – 0335	132
	06	0820 – 0935	132
	12	1420 – 1605	264
	18	2020 – 2135	132
Meso-scale Analysis/Forecast	00	0055 – 0205	51
	03	0355 – 0505	39
	06	0655 – 0805	39
	09	0955 – 1105	39
	12	1255 – 1405	51
	15	1555 – 1705	39
	18	1855 – 2005	39
	21	2155 – 2305	39
Meso-scale Ensemble Forecast	00	0150 – 0320	39
	06	0750 – 0920	39
	12	1350 – 1520	39
	18	1950 – 2120	39
Local Analysis/Forecast	00, 01, 02, 03, 04, 05, 06, 07, 08, 09, 10, 11, 12, 13, 14, 15, 16, 17, 18, 19, 20, 21, 22, 23	0035 – 0125, 0135 – 0225, 0235 – 0325, 0335 – 0425, 0435 – 0525, 0535 – 0625, 0635 – 0725, 0735 – 0825, 0835 – 0925, 0935 – 1025, 1035 – 1125, 1135 – 1225, 1235 – 1325, 1335 – 1425, 1435 – 1525, 1535 – 1625, 1635 – 1725, 1735 – 1825, 1835 – 1925, 1935 – 2025, 2035 – 2125, 2135 – 2225, 2235 – 2325, 2335 – 0025	10
Ocean Wave Forecast	00	0330 – 0400	132
	06	0930 – 1000	132
	12	1530 – 1600, 1840–1900	264
	18	2130 – 2200	132
Wave Ensemble	00	0445 – 0545	264

Forecast	12	1900 – 2000	264
Storm Surge Forecast	00 03 06 09 12 15 18 21	0200 – 0255 0500 – 0555 0800 – 0855 1100 – 1155 1400 – 1455 1700 – 1755 2000 – 2055 2300 – 2355	39 39 39 39 39 39 39 39
Asian-area Storm Surge Forecast	00 06 12 18	0340 – 0350 0940 – 0950 1540 – 1550 2140 – 2150	72 72 72 72
Global Ensemble Forecast (Typhoon/One-week)	00 06 12 18	0305 – 0355 0905 – 0935 1505 – 1555 2105 – 2135	264 132 264 132
Global Ensemble Forecast (Two-week)	00 12	0530 – 0630 1730 – 1830	264 – 432 264 – 432
Global Ensemble Forecast (One-month)	00 12	0655 – 0755 1855 – 1955 (every Tuesday and Wednesday)	432 – 816 432 – 816
Seasonal Ensemble Forecasts	00	1730 – 1910 (every 5 days)	(7 months)

4.2 Medium-range forecasting system (4 – 10 days)

4.2.1 Data assimilation, objective analysis and initialization

4.2.1.1 In operation

(1) Global Analysis (GA)

Hybrid four-dimensional variational (4D-Var) data assimilation involving the use of a Local Ensemble Transform Kalman Filter (LETKF ; Hunt et al. 2007) is employed in atmospheric analysis for the Global Spectral Model (GSM). Three-hour ensemble forecasting initialized with the LETKF is used in 4D-Var with the extended control variable method of Lorenc (2003) to create flow-dependent background error covariances, which are blended with climatological background error covariances. Analysis from 4D-Var is used to re-center LETKF ensemble analysis, and Figure 4.2.1-1 outlines the hybrid LETKF/4D-Var. An incremental method is adopted to improve computational efficiency using outer-loop iterations, with increments evaluated at a lower horizontal resolution (TL319). The increment is then interpolated and used to update the model trajectory at the original resolution (TL959), and the updated trajectory is used to refine the cost function for subsequent inner-loop iterations.

The Global Analysis (GA) is performed at 00, 06, 12 and 18 UTC. An early analysis with a short cut-off time is performed to prepare initial conditions for operational forecasting, and a cycle analysis with a long cut-off time is performed to maintain the quality of the global data assimilation system.

The specifications of the atmospheric analysis schemes are listed in Table 4.2.1-1 and 4.2.1-2.

The global land surface analysis system has been in operation since March 2000 to provide the initial conditions of land surface parameters for the GSM. The system includes daily global snow depth analysis, described in Table 4.2.1-3, to obtain appropriate initial conditions for snow coverage and depth.

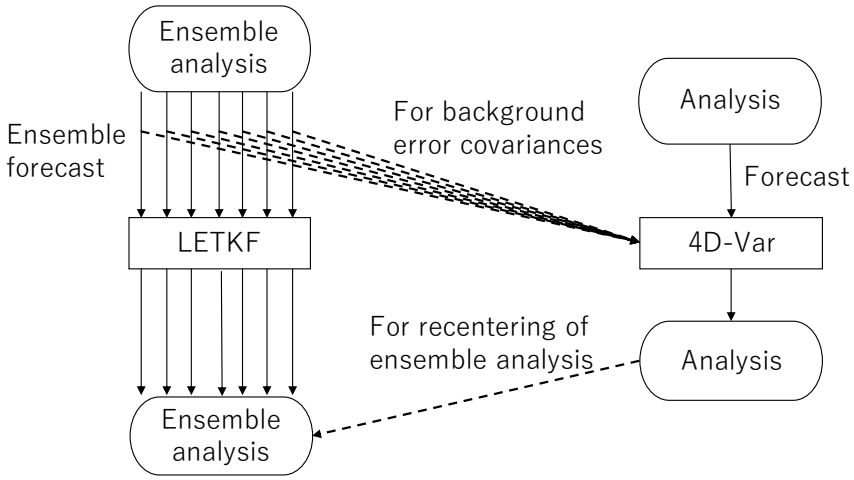

Figure 4.2.1-1. Hybrid LETKF/4D-Var

Table 4.2.1-1. Specifications of 4D-Var in GA

Analysis scheme	Incremental hybrid 4D-Var using LETKF
Data cut-off time	2 hours and 20 minutes for early run analysis at 00, 06, 12 and 18 UTC 11 hours and 50 minutes for cycle run analysis at 00 and 12 UTC 7 hours and 50 minutes for cycle run analysis at 06 and 18 UTC
First guess	6-hour forecast by the GSM
Domain configuration (Outer step)	Globe TL959, Reduced Gaussian grid, roughly equivalent to 0.1875° (20 km) [1920 (tropic) – 60 (polar)] x 960
(Inner step)	TL319, Reduced Gaussian grid, roughly equivalent to 0.5625° (55 km) [640 (tropic) – 60 (polar)] x 960
Vertical coordinates	σ-p hybrid
Vertical levels	100 forecast model levels up to 0.01 hPa + surface
Outer-loop iterations	2
Inner-loop iterations	Approx. 35
Control variables for climatological background error covariance	Relative vorticity, unbalanced divergence, unbalanced temperature, unbalanced surface pressure and natural logarithm of specific humidity
Covariance inflation for ensemble covariance	Adaptive multiplicative covariance inflation (as per LETKF application) Additional covariance inflation is applied to create vertical profiles for the horizontal global mean of standard deviation from ensemble covariances consistent with those from climatological background error covariances
Localization for ensemble covariance	Gaussian function. The localization scale for which the localization function is $1/\sqrt{e}$ is set to 800 km in the horizontal domain and a 0.8-scale height in the vertical domain.
Weighting for hybrid covariance	0.85 for climatological covariance and 0.15 for ensemble covariance under 50 hPa. Values approach 1 and 0 above 50 hPa, respectively.
Analysis variables	Wind, surface pressure, specific humidity and temperature

Observations (as of 31 December 2019)	SYNOP, METAR, SHIP, BUOY, TEMP, PILOT, Wind Profiler, AIREP, AMDAR, Typhoon Bogus; atmospheric motion vectors (AMVs) from Himawari-8, GOES-15, Meteosat-8, 11; MODIS polar AMVs from Terra and Aqua satellites; AVHRR polar AMVs from NOAA and Metop satellites; LEO-GEO AMVs; ocean surface wind from Metop-A, B, C/ASCAT; radiances from NOAA-15, 18, 19/ATOVS, Metop-A, B/ATOVS, Aqua/AMSU-A, DMSP-F17, 18/SSMIS, Suomi-NPP, NOAA-20/ATMS, GCOM-W/AMSR2, GPM-core/GMI, Coriolis/WindSat, FY-3C/MWRI, Megha-Tropiques/SAPHIR, Aqua/AIRS, Metop-A,B/IASI, Suomi-NPP, NOAA-20/CrIS, clear sky radiances from the water vapor channels (WV-CSRs) of Himawari-8, GOES-15, 16, Meteosat-8, 11; GNSS RO bending angle data from Metop-A, B/GRAS, COSMIC/IGOR, TerraSAR-X/IGOR; zenith total delay data from ground-based GNSS
Assimilation window	6 hours

Table 4.2.1-2. Specifications of the LETKF in GA

Data cut-off time	As per 4D-Var
First guess	Own 6-hour forecast
Domain configuration	As per 4D-Var inner step
Vertical coordinates	As per 4D-Var
Vertical levels	As per 4D-Var
Ensemble size	50 members
Perturbations to model physics	Stochastic perturbation of physics tendency
Initialization	Horizontal divergence adjustment based on analysis of surface pressure tendency (Hamrud et al. 2015)
Covariance inflation	Adaptive multiplicative covariance inflation
Localization	Gaussian function. The localization scale for which the localization function is $1/\sqrt{e}$ is set to 400 km in the horizontal domain (300 km for humidity-sensitive observations), a 0.4 scale height in the vertical domain (0.8 for surface pressure and ground-based GNSS zenith total-delay observations) and three hours in the temporal domain. For satellite radiance observations, the maximum of the square of the weighting function divided by its peak value and the Gaussian function with a $0.4\sqrt{2}$ scale height centered at the peak of the weighting function is used as the vertical localization function.
Re-centering	Ensemble analysis is re-centered so that the ensemble mean is consistent with 4D-Var.
Analysis variables	As per 4D-Var
Observation	As per 4D-Var, but without the use of Aqua/AIRS, Metop-A, B/IASI and Suomi-NPP, and NOAA-20/CrIS data
Assimilation window	As per 4D-Var

Table 4.2.1-3. Specifications of snow depth analysis in GA

Methodology	Two-dimensional Optimal Interpolation scheme
Domain and grids	Global, $1^\circ \times 1^\circ$ equal latitude-longitude grids
First guess	Derived from previous snow depth analysis and USAF/ETAC Global Snow Depth climatology (Foster and Davy 1988)
Data used	SYNOP snow depth data
Frequency	Daily

(2) Typhoon bogussing in GA

For typhoon forecasts over the western North Pacific, typhoon bogus data are generated to represent typhoon structures accurately in the initial field of forecast models. These data consist of information

on artificial sea-surface pressure and wind data around a typhoon. The structure is axi-asymmetric. Symmetric bogus profiles are first generated automatically based on the central pressure and 30-kt wind speed radius of typhoons. Asymmetric components are then retrieved from the first-guess fields and added to these profiles. Finally, the profiles are used as pseudo-observation data for GA.

4.2.1.2 Research performed in this field

(1) Operational Use of NOAA-20 ATMS and CrIS Radiance Data in JMA's Global NWP system

JMA began to assimilate data from the Advanced Technology Microwave Sounder (ATMS) and Cross-track Infrared Sounder (CrIS) onboard NOAA-20 into its global NWP system on 5 March 2019, in addition to Suomi National Polar-orbiting Partnership (Suomi-NPP) data. Quality control (QC) and error handling for the assimilation of NOAA-20/ATMS radiance data, such as channel selection, thinning distance, observation errors, rain/cloud detection and bias correction (static scan bias correction and variational bias correction) follow those implemented for Suomi-NPP/ATMS data assimilation (Hirahara et al. 2017). Currently, tropospheric temperature-sounding channels (6 – 9) and humidity-sounding channels (18 – 22) are assimilated. QC and error handling for the assimilation of NOAA-20/CrIS radiance data also follow those for Suomi-NPP/CrIS (Kamekawa and Kazumori 2017). The current assimilation involves 27 channels for temperature-sounding selected from the CO2 absorption band in the long-wave IR band (LWIR) as included in the disseminated 431 channel dataset. Assimilation experiments with the addition of NOAA-20/ATMS and CrIS data showed that NOAA-20 data quality is similar to or better than that of Suomi-NPP, and the additional use of NOAA-20 data improved the first-guess and forecast fields of temperature, humidity and geopotential height.

(2) Operational use of GOES-16 clear-sky radiance data in JMA's global NWP system

JMA began to assimilate GOES-16 CSR data on water vapor absorption bands (8, 9 and 10, with central wavelengths of 6.2, 6.9 and 7.3 μm, respectively) into its global NWP system on June 18 2019. This implementation was based on Himawari-8 CSR quality control involving the use of retrieved land surface temperature data, rather than first-guess skin temperature data, to improve the accuracy of simulated brightness temperature for surface-sensitive bands in particular (Okabe 2019). GOES-16 CSR quality evaluation showed that root mean squares of first-guess departure were as small as those for Himawari-8 CSR in areas of overlap with other geostationary satellites, and data quality was also considered similar. GOES-16 CSR data assimilation experiments showed a positive impact on WV field first-guess accuracy in the mid-to-upper troposphere, especially in the central part of the GOES-16 observation area. Humidity and geopotential height were improved in forecasts with periods up to two days for the low- and mid-latitudes of the troposphere.

(3) All-sky microwave radiance assimilation into JMA's global NWP system

JMA's all-sky microwave radiance assimilation scheme for microwave imagers and microwave water-vapor sounders (Kazumori and Kadowaki, 2017), which incorporates outer-loop iterations for

trajectory updates in the 4D-Var minimization process for effective assimilation of cloud and precipitation, was introduced into the operational global NWP system in December 2019. The RTTOV-SCATT (Radiative Transfer for TOVS; Bauer et al. 2006) model enables multiple-scattering radiative transfer calculation for microwave frequencies as part of the RTTOV-10 package adopted as an observation operator for all-sky assimilation processing. Observation error assignment based on the symmetric average of observations and first-guess cloud amounts (Geer and Bauer, 2011) is applied to handle the non-Gaussian distribution of observation errors. Biased data such as those caused by insufficient cloud representation in JMA's global forecast model (e.g., cold-sector bias) are removed, as the related observation error cannot be treated appropriately even if observation errors based on the symmetric cloud amount are considered. The all-sky assimilation scheme is applied to microwave imagers and microwave water-vapor sounders, most of which are previously applied clear-sky assimilation scheme and two of which are newly added. Data assimilation experiments indicated improvement of first-guess water vapor fields for the lower troposphere and the forecast field of geopotential height at 500 hPa, sea level pressure, and wind speed at 850 hPa up to a forecast range of 120 hours. The experiments also showed that average TC track forecast errors decreased over the whole forecast range up to 96 hours, and especially for the forecast range up to 72 hours, with statistical significance.

(4) Operational use of Metop-C ASCAT wind data in JMA's global NWP system

Metop-C ASCAT wind data were introduced into JMA's global NWP system on December 11 2019 (with an availability similar to that of Metop-A and B data), thereby increasing ocean vector wind (OVW) data coverage. As a result, OSEs showed improved temperature, low-level wind and water vapor data for tropical areas in the analysis field. The accuracy of 250 hPa wind speed forecasts and 850 hPa temperature forecasts also improved with radio sonde data as a reference.

(5) Ensemble member increase for flow-dependent background error covariances

Testing was performed with a greater number of ensemble members to create flow-dependent background error covariances in hybrid LETKF/4D-Var. The number of members was increased from 50 to 100 to reduce sampling errors, weighting for ensemble covariance was increased, and the horizontal/vertical localization function length scales in 4D-Var and LETKF were tuned. Retrospective experiments covering periods of at least a month in summer 2018 and winter 2018/19 showed increased ensemble spreads and reduced standard deviations of first-guess departures as compared to the current operational version. These upgrades are expected to be implemented in 2021.

4.2.2 Model

4.2.2.1 In operation

(1) Global Spectral Model (GSM)

The specifications of the operational Global Spectral Model (GSM1705; TL959L100) are summarized in Table 4.2.2-1.

The GSM forecasts with 00, 06 and 18 UTC initials were extended from 84 to 132 hours in June 2018 in association with the supercomputer system update. JMA runs the GSM four times a day at 00, 06 and 18 UTC with a forecast time of 132 hours and at 12 UTC with a forecast time of 264 hours.

Table 4.2.2-1 GSM 11-day forecast specifications

1. System	
Model (version)	Global Spectral Model (GSM1705)
Date of implementation	25 May 2017
2. Configuration	
Horizontal resolution (Grid spacing)	Spectral triangular 959 (TL959), reduced Gaussian grid system, roughly equivalent to 0.1875 × 0.1875˚ (20 km) in latitude and longitude
Vertical resolution (model top)	100 stretched sigma pressure hybrid levels (0.01 hPa)
Forecast length (initial time)	132 hours (00, 06, 18 UTC) 264 hours (12 UTC)
Coupling to ocean/wave/sea ice models	--
Integration time step	400 seconds
3. Initial conditions	
Data assimilation	Four-dimensional variational (4D-Var) method
4. Surface boundary conditions	
Treatment of sea surface	Climatological sea surface temperature with daily analysis anomaly Climatological sea ice concentration with daily analysis anomaly
Land surface analysis	Snow depth: two-dimensional optimal interpolation scheme Temperature: first guess Soil moisture: climatology
5. Other details	
Land surface and soil	Simple Biosphere (SiB) model
Radiation	Two-stream with delta-Eddington approximation for short wave (hourly) Two-stream absorption approximation method for long wave (hourly)
Numerical techniques	Spectral (spherical harmonic basis functions) in horizontal, finite differences in vertical Two-time-level, semi-Lagrangian, semi-implicit time integration scheme Hydrostatic approximation
Planetary boundary layer	Mellor and Yamada level-2 turbulence closure scheme Similarity theory in bulk formulae for surface layer
Convection	Prognostic Arakawa-Schubert cumulus parameterization
Cloud	PDF-based cloud parameterization
Gravity wave drag	Longwave orographic drag scheme (wavelengths > 100 km) mainly for stratosphere Shortwave orographic drag scheme (wavelengths approx.. 10 km) for troposphere only Non-orographic spectral gravity wave forcing scheme
6. Further information	
Operational contact point	globalnwp@naps.kishou.go.jp

System documentation URL	http://www.jma.go.jp/jma/jma-eng/jma-center/nwp/nwp-top.htm

4.2.2.2 Research performed in this field

(1) Upgrade of the GSM

JMA plans to upgrade its Global Spectral Model (GSM) in 2020 with revised physics parameterization schemes (such as those relating to surface drag processes, land surface processes, surface albedo and stratocumulus over sea ice) to improve forecasting for the Northern Hemisphere and elsewhere.

4.2.3 Operationally available NWP products

The model output products shown below from the GSM are disseminated through JMA's radio facsimile broadcast (JMH) service, GTS and the Global Information System Centre (GISC) Tokyo website.

Table 4.2.3-1 List of facsimile charts transmitted via the GTS and JMH

The contour lines (upper-case letters) are: D: dew-point depression (T - T_d); E: precipitation; H: geopotential height; J: wave height; O: vertical velocity (ω); P: sea level pressure; T: temperature; W: isotach wind speed; Z: vorticity; δ: anomaly from climatology; μ: average over time. The other symbols are: a: wind arrows; b: observation plots; d: hatch for dewpoint depression < 3 K; g: arrows for prevailing wave direction; j: jet axis; m: wave period in digits; t: temperature in digits; x: streamlines. The subscripts in the table indicate: $_{srf}$: surface; $_{trp}$: tropopause; digit (ex. $_{500}$) pressure in hPa. The superscripts indicate dissemination channels and time: ^{G}: sent to GTS; ^{J}: sent to JMH; ^{12}: for 12 UTC only; ^{5}: statistics for pentad sent once per five days for 00 UTC; ^{m}: statistics for the month sent monthly for 00 UTC.

<table>
<tr><td rowspan="2">Model</td><td rowspan="2">Area</td><td></td><td colspan="8">Forecast Time [h]</td></tr>
<tr><td>Analysis</td><td>12</td><td>24</td><td>36</td><td>48</td><td>72</td><td>96
120</td><td>144
168
192</td></tr>
<tr><td rowspan="2">GSM</td><td>Asia</td><td>$HWbt_{300}^{G}$
$HTbt_{500}^{GJ}$
$HTbd_{700}^{G}$
$HTbd_{850}^{GJ}$</td><td></td><td>EP_{srf}^{G}</td><td></td><td colspan="2">HZ_{500}^{G}
$Ta_{850}O_{700}^{G12}$
EP_{srf}^{GJ}</td><td>EP_{srf}^{GJ12}</td><td></td></tr>
<tr><td>East Asia</td><td>HZ_{500}^{G}
$Ta_{850}O_{700}^{G}$</td><td></td><td colspan="3">HZ_{500}^{GJ}
$Dd_{700}T_{500}^{GJ}$
$Ta_{850}O_{700}^{GJ}$
EPa_{srf}^{GJ}</td><td></td><td colspan="2">HZ_{500}^{G12}
$P_{srf}T_{850}^{G12}$</td></tr>
<tr><td rowspan="4"></td><td>Asia-Pacific</td><td>$HWajt_{200}H_{trp}^{G}$
$HWat_{250}^{G}$</td><td></td><td colspan="2">$HTWa_{250}^{G}$
$HTWa_{500}^{G}$</td><td></td><td></td><td></td><td></td></tr>
<tr><td>NW Pacific</td><td>x_{200}^{G}
x_{850}^{G}</td><td></td><td colspan="2">x_{200}^{G}
x_{850}^{G}</td><td>x_{200}^{G}
x_{850}^{G}</td><td></td><td></td><td></td></tr>
<tr><td>N Hem.</td><td>HT_{500}^{G12}</td><td></td><td></td><td></td><td></td><td></td><td></td><td></td></tr>
<tr><td></td><td></td><td></td><td></td><td></td><td></td><td></td><td></td><td></td><td></td></tr>
<tr><td rowspan="2">Ocean Wave</td><td>Japan</td><td>$Jabgm_{srf}^{GJ}$</td><td></td><td></td><td></td><td></td><td></td><td></td><td></td></tr>
<tr><td>NW Pacific</td><td>$Jbgm_{srf}^{GJ}$</td><td colspan="2">Jgm_{srf}^{J}</td><td></td><td colspan="2">Jgm_{srf}^{J}</td><td></td><td></td></tr>
</table>

Table 4.2.3-2 List of GPV products (GRIB2) distributed via the GISC Website

Symbols: H: geopotential height; U: eastward wind; V: northward wind; W: wind speed; G: gusts; T: temperature; R: relative humidity; O: vertical velocity (ω); Z: vorticity; X: stream function; Y: velocity potential; Di: relative divergence; P: pressure; Ps: sea level pressure; E: rainfall; N: total cloud cover; Ch: high cloud cover; Cm: middle cloud cover; Cl: low cloud cover. The prefixes μ and σ represent the average and standard deviations of ensemble prediction results, respectively. The prefix ρ represents the probability of ensemble prediction results, and parentheses represent probability thresholds.

Model	GSM	GSM
Area and resolution	Whole globe, Region II 0.25° × 0.25° (surface), 0.5° × 0.5° (surface, isobar level)	Whole globe, Region II 1.25° × 1.25°
Elements	10 hPa: H, U, V, T, R, O 20 hPa: H, U, V, T, R, O 30 hPa: H, U, V, T, R, O 50 hPa: H, U, V, T, R, O 70 hPa: H, U, V, T, R, O 100 hPa: H, U, V, T, R, O 150 hPa: H, U, V, T, R, O 200 hPa: H, U, V, T, R, O, X, Y 250 hPa: H, U, V, T, R, O 300 hPa: H, U, V, T, R, O 400 hPa: H, U, V, T, R, O 500 hPa: H, U, V, T, R, O, Z 600 hPa: H, U, V, T, R, O 700 hPa: H, U, V, T, R, O 800 hPa: H, U, V, T, R, O 850 hPa: H, U, V, T, R, O, X, Y 900 hPa: H, U, V, T, R, O 925 hPa: H, U, V, T, R, O 950 hPa: H, U, V, T, R, O 975 hPa: H, U, V, T, R, O 1,000 hPa: H, U, V, T, R, O Surface: U, V, T, R, P, Ps, E, N, Ch, Cm, Cl	10 hPa: H, U, V, T 20 hPa: H, U, V, T 30 hPa: H, U, V, T 50 hPa: H, U, V, T 70 hPa: H, U, V, T 100 hPa: H, U, V, T 150 hPa: H, U, V, T 200 hPa: H, U, V, T, X, Y 250 hPa: H, U, V, T, Z, Di 300 hPa: H, U, V, T, R, O 400 hPa: H, U, V, T, R, O 500 hPa: H, U, V, T, R, O, Z 600 hPa: H, U, V, T, R, O 700 hPa: H, U, V, T, R, O, Z, Di 850 hPa: H, U, V, T, R, O, X, Y 925 hPa: H, U, V, T, R, O, Z, Di 1,000 hPa: H, U, V, T, R, O Surface: U, V, T, R, Ps, E
Forecast hours	0 – 84 every 3 hours, 90 – 264 every 6 hours (12 UTC)	0 – 132 every 6 hours, 144 – 264 every 12 hours (12 UTC)
Initial times	00 UTC, 06 UTC, 12 UTC, 18 UTC	00 UTC, 06 UTC, 12 UTC, 18 UTC

Model	Global Ensemble Forecast (One-week)
Area and resolution	Whole globe 1.25° × 1.25°
Levels and elements	250 hPa: μU, μV, σU, σV 500 hPa: μH, σH 850 hPa: μU, μV, σU, σV, μT, σT, μW, σW, ρT (±1, ±1.5, ±2 standard deviation with respect to reanalysis climatology) 1,000 hPa: μH, σH Surface: μP, σP, ρE (1, 5, 10, 25, 50, 100 mm/24hours), ρW (10, 15, 25 m/s), ρG (10, 15, 25 m/s),
Forecast hours	0 – 264 every 12 hours
Initial times	00 UTC and 12 UTC

Table 4.2.3-3 List of GPV products (GRIB) distributed via the GISC website and the GTS

Symbols: D: dew-point depression; E: precipitation; G: prevailing wave direction; H: geopotential height; J: wave height; M: wave period; O: vertical velocity (ω); P: sea level pressure; R: relative humidity; T: temperature; U: eastward wind; V: northward wind; X: stream function; Y: velocity potential; Z: vorticity;
The prefixes μ and σ represent the average and standard deviations of ensemble prediction results, respectively. The symbols °, *, ¶, §, ‡ and † indicate limitations on forecast hours or initial times as shown in the notes below.

Model	GSM	GSM	GSM
Destination	GTS, GISC	GTS, GISC	GTS, GISC
Area and resolution	Whole globe, 1.25° × 1.25°	20°S – 60°N, 60°E – 160°W 1.25° × 1.25°	Whole globe, 2.5° × 2.5°
Levels and elements	10 hPa: H, U, V, T 20 hPa: H, U, V, T 30 hPa: H, U, V, T 50 hPa: H, U, V, T 70 hPa: H, U, V, T 100 hPa: H, U, V, T 150 hPa: H, U, V, T 200 hPa: H, U, V, T, X, Y 250 hPa: H, U, V, T 300 hPa: H, U, V, T, R, O 400 hPa: H, U, V, T, R, O 500 hPa: H, U, V, T, R, O, Z 600 hPa: H, U, V, T, R, O 700 hPa: H, U, V, T, R, O 850 hPa: H, U, V, T, R, O, X, Y 925 hPa: H, U, V, T, R, O 1,000 hPa: H, U, V, T, R, O Surface: P, U, V, T, R, E†	10 hPa: H, U, V, T 20 hPa: H, U, V, T 30 hPa: H, U, V, T 50 hPa: H, U, V, T 70 hPa: H, U, V, T 100 hPa: H, U, V, T 150 hPa: H, U, V, T 200 hPa: H§, U§, V§, T§, X, Y 250 hPa: H, U, V, T 300 hPa: H, U, V, T, D 400 hPa: H, U, V, T, D 500 hPa: H§, U§, V§, T§, D§, Z 700 hPa: H§, U§, V§, T§, D§, O 850 hPa: H§, U§, V§, T§, D§, O, X, Y 925 hPa: H, U, V, T, D, O 1,000 hPa: H, U, V, T, D Surface: P¶, U¶, V¶, T¶, D¶, E¶	10 hPa: H*, U*, V*, T* 20 hPa: H*, U*, V*, T* 30 hPa: H°, U°, V°, T° 50 hPa: H°, U°, V°, T° 70 hPa: H°, U°, V°, T° 100 hPa: H°, U°, V°, T° 150 hPa: H*, U*, V*, T* 200 hPa: H, U, V, T 250 hPa: H°, U°, V°, T° 300 hPa: H, U, V, T, D*‡ 400 hPa: H*, U*, V*, T*, D*‡ 500 hPa: H, U, V, T, D*‡ 700 hPa: H, U, V, T, D 850 hPa: H, U, V, T, D 1,000 hPa: H, U*, V*, T*, D*‡ Surface: P, U, V, T, D*‡, E†
Forecast hours	0 – 84 every 6 hours and 96 – 192 every 12 hours for 12 UTC † Except analysis	0 – 84 every 6 hours § Additional 96 – 192 every 24 hours for 12 UTC ¶ 0 – 192 every 6 hours for 12 UTC	0 – 72 every 24 hours and 96 – 192 every 24 hours for 12 UTC ° 0 – 120 for 12 UTC † Except analysis * Analysis only
Initial times	00 UTC, 06 UTC, 12 UTC, 18 UTC	00 UTC, 06 UTC, 12 UTC, 18 UTC	00 UTC, 12 UTC ‡ 00 UTC only

Model	Global Ensemble Forecast (One-week)	Ocean Wave Model
Destination	GISC	GTS, GISC
Area and resolution	Whole globe, 2.5° × 2.5°	75°S – 75°N, 0°E – 359.5°E 0.5° × 0.5°
Levels and elements	250 hPa: μU, μV, σU, σV 500 hPa: μH, σH 850 hPa: μU, μV, μT, σU, σV, σT 1,000 hPa: μH, σH Surface: μP, σP	Surface: J, M, G
Forecast hours	0 – 192 every 12 hours	0 – 84 every 6 hours, 96 – 192 every 12 hours for 12 UTC
Initial times	00 UTC and 12 UTC	00 UTC, 06 UTC, 12 UTC, 18 UTC

4.2.4 Operational techniques for application of NWP products

4.2.4.1 In operation

(1) Forecast guidance

The application techniques for both the medium- and short-range forecasting systems are described in 4.3.4.1 (1).

4.2.4.2 Research performed in this field

4.2.5 Ensemble Prediction System (EPS)

4.2.5.1 In operation

The Global EPS (GEPS) has been in operation for medium- to extended-range forecasting since the first quarter of 2017, supporting seamlessly the issuance of five-day tropical cyclone (TC) forecasts, one-week forecasts, early warning information on extreme weather and one-month forecasts. The specifications of GEPS for the first 11 days of forecasts are shown in Table 4.2.5-1. The system involves the application of 1 control forecast and 26 perturbed forecasts. Initial perturbations are generated using a combination of the Local Ensemble Transform Kalman Filter approach (LETKF; Hunt et al. 2007) and the singular vector (SV) method (Buizza and Palmer 1995). The specifications of LETKF are shown in Table 4.2.5-2. Using this filtering technique, a six-hour cycle data assimilation system is implemented to generate initial perturbations representing flow-dependent uncertainty in the initial conditions. The tangent-linear and adjoint models used for SV computation are lower-resolution versions of those used in the 4D-Var data assimilation system for the GSM until May 2017. The moist total energy norm (Ehrendorfer et al. 1999) is employed for the metrics of perturbation growth. The forecast model used in the EPS is a low-resolution version of the GSM1603E (see Table 4.2.5-1). Accordingly, the dynamical framework and physical processes involved are slightly older versions of those in the high-resolution GSM. A stochastic physics scheme (Palmer et al. 2009) is used in GEPS in consideration of model uncertainties associated with physical parameterizations.

Unperturbed initial condition is performed by interpolating the analyzed field in global analysis (see 4.2.1.1). The sea surface temperature (SST) analysis value is used as a lower-boundary condition and prescribed using the persisting anomaly from the climatological value, which means that the anomalies shown from analysis for the initial time are fixed during time integration. The sea ice concentration analysis value is also prescribed using the persisting anomaly. A perturbation technique for SST that is designed to represent uncertainty in the prescribed SST is applied to GEPS as a surface boundary perturbation.

Table 4.2.5-1 Global EPS specifications for the first 11 days of forecasts

1. Ensemble system	
Ensemble (version)	Global EPS (GEPS)
Date of implementation	19 January 2017
2. EPS configuration	
Model (version)	Global Spectral Model (GSM1603E)
Horizontal resolution/grid spacing	Spectral triangular 479 (TL479), reduced Gaussian grid system, roughly equivalent to 0.375 × 0.375° (40 km) in latitude and longitude
Vertical resolution (model top)	100 stretched sigma pressure hybrid levels (0.01 hPa)
Forecast length (initial time)	11 days (00, 12 UTC) 132 hours (06, 18 UTC)
Members	1 unperturbed control forecast and 26 perturbed ensemble members
Coupling to ocean/wave/sea ice models	--
Integration time step	720 seconds
Additional comments	Forecasts from initial times at 06 and 18 UTC are issued when either of the following conditions is satisfied at the initial times: · A tropical cyclone (TC) of tropical storm (TS) intensity or higher is present in the RSMC Tokyo – Typhoon Center's area of responsibility (0 – 60°N, 100°E – 180°). · A TC is expected to reach or exceed TS intensity in the area within the next 24 hours.
3. Initial conditions and perturbations	
Initial perturbation strategy	Singular vectors (SVs) and LETKF
Optimization time in forecast	Among three targeted SV areas: 48 hours for Northern Hemisphere (30° – 90°N) 24 hours for Tropics (30°S – 30°N) 48 hours for Southern Hemisphere (90° – 30°S)
Horizontal resolution of perturbations	SVs: Spectral triangular 63 (TL63), reduced Gaussian grid system, roughly equivalent to 2.8125 × 2.8125° (270 km) in latitude and longitude Perturbations from LETKF: Spectral triangular 319 (TL319), reduced Gaussian grid system, roughly equivalent to 0.5625 ×0.5625° (55 km) in latitude and longitude
Initial perturbation area	Global
Data assimilation method for control analysis	Four-dimensional variational (4D-Var) for Global Analysis (GA) Control analysis based on interpolation of high-resolution GA (TL959)
Initial conditions for perturbed members	Addition of perturbations to control analysis (SV-based components in +/- pairs)
Additional comments	LETKF-based perturbations are produced using six-hour forecasts starting from the previous LETKF cycle.
4. Model uncertainty perturbations	
Model physics perturbations	Stochastic perturbation of physics tendency
Model dynamics perturbations	--
Additional comments	· Identical model versions for all ensemble members · Above model uncertainty perturbations not applied to control forecasting

5. Surface boundary perturbations	
Sea surface temperature perturbations	Perturbations representing climatological distribution of analysis and forecast error of prescribed SST sampled from past realizations of analysis increment and forecast error of SST in the same season
Soil moisture perturbations	--
Surface wind stress/roughness perturbations	--
Other surface perturbations	--
Additional comments	The above surface perturbations are not applied to the control forecast.
6. Other model details	
Surface boundary conditions	
Treatment of sea surface	Climatological sea surface temperature with daily analysis anomaly Climatological sea ice concentration with daily analysis anomaly
Land surface analysis	Snow depth: two-dimensional optimal interpolation scheme Temperature: first guess Soil moisture: climatology
Model dynamics and physics	
Land surface and soil	Simple Biosphere (SiB) model
Radiation	Two-stream with delta-Eddington approximation for shortwave (hourly) Two-stream absorption approximation method for longwave (hourly)
Numerical techniques	Spectral (spherical harmonic basis functions) in horizontal, finite differences in vertical Two-time-level, semi-Lagrangian, semi-implicit time integration scheme Hydrostatic approximation
Planetary boundary layer	Mellor and Yamada level-2 turbulence closure scheme Similarity theory in bulk formulae for surface layer
Convection	Prognostic Arakawa-Schubert cumulus parameterization
Cloud	PDF-based cloud parameterization
Gravity wave drag	Longwave orographic drag scheme (wavelengths > 100 km) mainly for stratosphere Shortwave orographic drag scheme (wavelengths approx. 10 km) for troposphere only Non-orographic spectral gravity wave forcing scheme
7. Products	
Method of calculation (if not unique)	
Other specifications as necessary	Products of forecasts from initial times at 06 and 18 UTC are not externally provided on an operational basis.
8. Further information	
Operational contact	globalnwp@naps.kishou.go.jp
System documentation URL	http://www.jma.go.jp/jma/jma-eng/jma-center/nwp/nwp-top.htm

Table 4.2.5-2 LETKF specifications

Model name (version)	Global Spectral Model (GSM1705)
Horizontal resolution	Spectral triangular 319 (TL319), reduced Gaussian grid system, roughly equivalent to 0.5625° ×0.5625° (55 km) in latitude and longitude
Vertical resolution (model top)	100 unevenly spaced hybrid levels (0.01 hPa)
Analysis time	00, 06, 12, 18 UTC
Ensemble size	50 members
Data cut-off time	2 hours and 20 minutes
First guess	Own 6-hour forecast

Analysis variables	Wind, surface pressure, specific humidity and temperature
Observation (as of 31 December 2019)	The same as Global Analysis (GA) shown in Table 4.2.1-1, except that Aqua/AIRS, Metop-A,B/IASI and Suomi-NPP, NOAA-20/CrIS are not used.
Assimilation window	6 hours
Perturbations to model physics	Stochastic perturbation of physics tendency
Initialization	Hamrud et al. (2015)
Covariance inflation	Adaptive multiplicative covariance inflation
Other characteristics	A total of 50 analyses are re-centered so that their ensemble mean is consistent with the Global Analysis (GA). A total of 26 of these 50 are used to generate GEPS initial perturbations.

4.2.5.2 Research performed in this field

(1) 2020 GEPS upgrade research

JMA plans to upgrade GEPS in 2020 to incorporate recent GSM developments, a two-tiered sea surface temperature (SST) approach (Takakura and Komori, 2020) and a direct application of initial perturbations from the hybrid data cycle of the global NWP system. Sharing of the same forecast model as the GSM (also scheduled to be upgraded simultaneously) will lead to updating with GSM developments made since the 2017 introduction of GEPS. The amplitude of singular vector (SV)-based initial perturbations targeted in the high- and mid-latitudes of both hemispheres will also be reduced by 8.7% to mitigate over-dispersiveness in 500-hPa geopotential height forecasts with lead times of up to four days. SVs located in desert areas in low latitudes will be removed, as irrational humidity perturbations are observed over climatologically dry areas. To verify the performance of these modifications for medium-range forecasting with lead times of up to 11 days, retrospective experiments covering periods of at least three months in summer 2018 and winter 2017/18 were conducted. The results showed improved ensemble mean forecast RMSEs for several elements, including 850 hPa temperature, 500 hPa geopotential height and 200 hPa winds, for both seasons. Winter Brier skill scores for forecasts of precipitation in Japan were also improved.

4.2.5.3 Operationally available EPS products

See 4.2.3.

4.3 Short-range forecasting system (0 – 72 hrs)

4.3.1 Data assimilation, objective analysis and initialization

4.3.1.1 In operation

(1) Meso-scale Analysis (MA)

Meso-scale Analysis (MA) produces initial conditions for the Meso-Scale Model (MSM, 4.3.2.1 (1)).

In March 2002, a four-dimensional variational (4D-Var) scheme was introduced as the data assimilation approach for MA (Ishikawa and Koizumi 2002). Following the upgrade of the MSM forecast model to a non-hydrostatic type, MA was replaced by a non-hydrostatic model-based 4D-Var system known as the JMA non-hydrostatic model (JMA-NHM; Saito et al. 2006, 2007) variational data assimilation (JNoVA; Honda et al. 2005) system in April 2009. A further upgraded forecast model called ASUCA (Aranami et al. 2015) has been employed since February 2017, and a 4D-Var system based on ASUCA is currently under development. The specifications of MA are described in Table 4.3.1-1.

Table 4.3.1-1 Specifications of the Meso-scale Analysis (MA)

Analysis time	00, 03, 06, 09, 12, 15, 18 and 21 UTC
Analysis scheme	Incremental 4D-Var using a nonlinear forward model in the inner step with low resolution
Data cut-off time	50 minutes for analysis at 00, 03, 06, 09, 12, 15, 18 and 21 UTC
First guess	3-hour forecast produced by JMA-NHM
Domain configuration (Outer step) (Inner step)	Japan and its surrounding area Lambert projection; 5 km at 60°N and 30°N, 817 × 661 Grid point (1, 1) is at the northwest corner of the domain. Grid point (565, 445) is at 140°E, 30°N. Lambert projection; 15 km at 60°N and 30°N, 273 × 221 Grid point (1, 1) is at the northwest corner of the domain. Grid point (189, 149) is at 140°E, 30°N.
Vertical coordinate	z-z* hybrid
Vertical levels	(Outer step) 48 levels up to 22 km (Inner step) 38 levels up to 22 km
Analysis variables	Wind, potential temperature, surface pressure and pseudo-relative humidity
Observations (as of 31 December 2018)	SYNOP, SHIP, BUOY, TEMP, PILOT, Wind Profiler, Weather Doppler radar (radial velocity, reflectivity), AIREP, AMDAR, Typhoon Bogus; AMVs from Himawari-8; ocean surface wind from Metop-A, B/ASCAT; radiances from NOAA-15, 18, 19/ATOVS, Metop-A, B/ATOVS, Aqua/AMSU-A, DMSP-F17, 18/SSMIS, GCOM-W/AMSR2, GPM-core/GMI, WV-CSR of Himawari-8; radar-raingauge analyzed precipitation; precipitation retrievals from DMSP-F17, 18/SSMIS, GCOM-W/AMSR2, GPM-core/GMI, GPM-core/DPR; GNSS RO refractivity data from Metop-A, B/GRAS, COSMIC/IGOR, TerraSAR-X/IGOR, TanDEM-X/IGOR; total precipitable water vapor from ground-based GNSS
Assimilation window	3 hours
System documentation URL	http://www.jma.go.jp/jma/jma-eng/jma-center/nwp/nwp-top.htm

(2) Typhoon bogussing of the MA

The method employed is essentially as per that used for GA (see 4.2.1.1 (2)).

(3) Local Analysis (LA)

Local Analysis (LA) produces initial conditions for the Local Forecast Model (LFM, 4.3.2.1 (2)). Its operation started in August 2012. To provide high-resolution initial conditions that are suitable for LFM, LA is designed to allow rapid production and frequent updating of analysis with a grid spacing

of 5 km. In each LA run, an analysis cycle with hourly three-dimensional variational (3D-Var) data assimilation is executed for the previous three hours to incorporate information from newly received observational data in each case. The analysis cycle was originally based on JMA-NHM (Saito et al. 2006, 2007) and the 3D-Var version of JNoVA (Honda et al. 2005), which was replaced by the new-generation 3D-Var version based on ASUCA in January 2015 (Aranami et al. 2015). The capacity of high-resolution NWP to capture small-scale variations in topography is expected to help reduce representativeness errors in the assimilation of surface observations. In association, LA also assimilates Automated Meteorological Data Acquisition System (AMeDAS) data in order to appropriately reflect the effects of local-scale environments near the surface. The specifications of LA are described in Table 4.3.1-2.

Table 4.3.1-2 LA specifications

Analysis time	00, 01, 02, 03, 04, 05, 06, 07, 08, 09, 10, 11, 12, 13, 14, 15, 16, 17, 18, 19, 20,21, 22 and 23 UTC
Analysis cycle	The three-hour analysis cycle repeats hourly assimilation with 3D-Var and one-hour forecasts.
Data cut-off time	30 minutes for analysis at 00, 01, 02, 03, 04, 05, 06, 07, 08, 09, 10, 11, 12, 13, 14, 15, 16, 17, 18, 19, 20, 21, 22 and 23 UTC
First guess	Initial fields produced by the latest MSM
Domain configuration	Japan and its surrounding area Lambert projection; 5 km at 60°N and 30°N, 633 × 521 Grid point (1, 1) is at the northwest corner of the domain. Grid point (449, 361) is at 140°E, 30°N
Vertical coordinate	z-z^* hybrid
Vertical levels	48 levels up to 22 km
Analysis variables	Wind, potential temperature, surface pressure, pseudo-relative humidity, skin temperature, ground temperature and soil moisture
Observations (as of 31 December 2018)	SYNOP, SHIP, BUOY, AMeDAS, TEMP, PILOT, Wind Profiler, Weather Doppler radar (radial velocity, reflectivity), AIREP, AMDAR; AMVs from Himawari-8; radiances from NOAA-15, 18, 19/ATOVS, Metop-A, B/ATOVS, Aqua/AMSU-A, DMSP-F17, 18/SSMIS, GCOM-W/AMSR2, GPM-core/GMI, WV-CSRs of Himawari-8; soil moisture from GCOM-W/AMSR2, Metop-A B/ASCAT; total precipitable water vapor from ground-based GNSS
System documentation URL	http://www.jma.go.jp/jma/jma-eng/jma-center/nwp/nwp-top.htm

4.3.1.2 Research performed in this field

(1) Operational use of surface-sensitive clear-sky radiance data in JMA's mesoscale NWP system

JMA began to assimilate Himawari-8 surface-sensitive band 9 and 10 (6.9 and 7.3 μm) clear-sky radiance (CSR) data in its mesoscale NWP system on March 26 2019 in addition to band 8 (6.2 μm) CSR data. In the quality control process, the radiative transfer calculation introduced into JMA's global NWP system (which uses the land surface emissivity atlas and retrieved land surface temperatures from the window channel (10.8 μm; band 13) CSR (Okabe 2019)) was applied for better accuracy of simulated brightness temperature, especially for surface-sensitive bands. Positive impacts from these CSRs on WV field accuracy for the first guess in the MSM were found in an assimilation experiment, which also revealed improved precipitation forecast scores.

(2) Bias correction for aircraft temperature data in JMA's mesoscale NWP system

Correction for aircraft temperature bias was introduced into JMA's operational mesoscale data assimilation system on March 26 2019. Bias estimation is based on monthly statistics of first-guess (FG) departures for individual aircraft tail numbers and flight levels over the previous month (Sako 2010). The correction was found to reduce positive biases and root mean square errors of temperature above 300 hPa.

(3) Enhanced use of ground-based GNSS data in JMA's mesoscale NWP system

Precipitable water vapor (PWV) data derived from ground-based GNSS in rainy conditions have been used in JMA's operational mesoscale data assimilation system since March 26 2019.

JMA previously reported that PWV data derived from ground-based GNSS in rainy conditions (referred to as rain data) had a negative bias against the first guess in mesoscale analysis.

As a result, data from areas with approximately 1.5 mm/hour of rainfall were rejected in quality control and not used in mesoscale analysis. However, a review based on PWV data collected since 2015 indicated that rain data exhibit no bias in any season. As the mesoscale model has been improved, negative biases were reduced and rain data are now considered appropriate for use with the current mesoscale data assimilation system.

(4) Operational use of ocean vector wind (OVW) data from ASCAT 12.5 km coastal wind information in JMA's mesoscale NWP system

Ocean vector wind (OVW) data for mesoscale NWP analysis were switched from ASCAT 25 km winds to ASCAT 12.5 km coastal winds (Verhoef et al. 2012) on March 26 2019. The quality control settings and parameters for coastal wind data are identical to those for 25 km OVWs, and spatial thinning of 0.5 degrees (approximately 50 km) is applied to both products. As the target area of the JMA mesoscale NWP system includes various islands and coastal regions, the use of coastal wind data increases sea-surface coverage in coastal regions. OSEs showed improved precipitation scores and typhoon track prediction based on OVW data from ASCAT 12.5 km coastal wind information.

4.3.2 Model

4.3.2.1 In operation

(1) Meso-Scale Model (MSM)

The MSM operated by JMA since March 2001 plays major roles in disaster prevention and aviation forecasting. JMA-NHM (Saito et al. 2006, 2007) was adopted for the MSM in September 2004, and 15- or 33-hour forecasts have been provided every three hours (i.e., eight times a day) since May 2007. The forecast domain was expanded in March 2013. The forecast range at all the initial times was extended to 39 hours in May 2013. The ASUCA forecast model (Ishida et al. 2009, 2010) was

introduced in February 2017, and the number of vertical layers was increased from 48 to 76 for enhanced resolution. The forecast range at the initial times of 00 and 12 UTC was extended to 51 hours in March 2019. MSM specifications are listed in Table 4.3.2-1.

Table 4.3.2-1 MSM specifications

1. System	
System	Meso-scale model
Date of implementation	1 March 2001
2. Configuration	
Domain	Japan and its surrounding area Lambert projection, 817 × 661 grid points
Horizontal resolution	5 km at 60°N and 30°N (standard parallels)
Vertical levels	76
Model top	22 km
Forecast length	51 hours (00, 12 UTC), 39 hours (03, 06, 09, 15, 18, 21 UTC)
Runs per day (times in UTC)	8 (00, 03, 06, 09, 12, 15, 18 and 21 UTC)
Coupling to ocean/wave/sea ice models	None
Integration time step	100/3 seconds (3-stage Runge-Kutta method)
3. Surface boundary conditions	
Sea-surface temperature	Analyzed SST and sea-ice distribution
Land surface analysis	Climatological values of evaporability, roughness length and albedo Snow cover analysis over Japan using a land surface model
4. Lateral boundary conditions	
Model providing lateral boundary conditions	GSM
Lateral boundary condition update frequency	4 times/day 00 – 45-hour GSM forecasts initialized at 00/06/12/18 UTC for (03, 06)/(09, 12)/(15, 18)/(21, 00) UTC forecasts
5. Other details	
Soil scheme	Ground temperature prediction using an eight-layer ground model Evaporability prediction initialized using climatological values depending on location and season
Radiation	Short wave: two-stream with delta-Eddington approximation (every 15 minutes) Long wave: two-stream absorption approximation method (every 15 minutes)
Large-scale dynamics	Finite volume method with Arakawa-C-type staggered coordinates, horizontally explicit and vertically implicit time integration scheme, and combined third- and first-order upwind horizontal finite difference schemes in flux form with a limiter as proposed by Koren (1993) in advection treatment for monotonicity, time-splitting of vertical advection Fully compressible non-hydrostatic equations
Boundary layer	Mellor-Yamada-Nakanishi-Niino Level-3 scheme Similarity theory adopted for surface boundary layer
Convection	Kain-Fritsch convection scheme
Cloud/microphysics	Three-ice bulk cloud microphysics Consideration of PDF-based cloud distribution in microphysics Time splitting of vertical advection for water substances, cloud water and cloud cover diagnosed using a partial condensation scheme
Orography	Mean orography smoothed to eliminate shortest-wave components
Horizontal diffusion	None
Gravity wave drag	None
6. Further information	

System documentation URL	http://www.jma.go.jp/jma/jma-eng/jma-center/nwp/nwp-top.htm

(2) Local Forecast Model (LFM)

JMA has operated LFM since August 2012. The model has a 2-km horizontal grid spacing and 58 vertical layers up to a height of approximately 20 km above the surface with a nine-hour forecast range, and is designed to produce detailed forecasts with emphasis on predicting localized and short-lived severe events. The main purposes of the LFM are to provide very short-range forecasts and to allow rapid and frequent forecast updates based on initial conditions with the latest observations assimilated via LA (4.3.1.1 (3)). The forecast domain was expanded to cover Japan and its surrounding areas, and the update frequency was enhanced to every hour in May 2013. The ASUCA forecast model was introduced in January 2015 (Aranami et al. 2015), replacing the previous JMA-NHM (Saito et al. 2006, 2007). The forecast range for all the initial times was extended to 10 hours in March 2019. The specifications of the LFM are listed in Table 4.3.2-2.

Table 4.3.2-2 LFM specifications

1. System	
System	Local Forecast Model
Date of implementation	30 August 2012
2. Configuration	
Domain	Japan and its surrounding area Lambert projection, 1,581 × 1,301 grid points
Horizontal resolution	2 km at 60°N and 30°N (standard parallels)
Vertical levels	58
Model top	20 km
Forecast length	10 hours
Runs per day (times in UTC)	24 (00, 01, 02, 03, 04, 05, 06, 07, 08, 09, 10, 11, 12, 13, 14, 15, 16, 17, 18, 19, 20, 21, 22 and 23 UTC)
Coupling to ocean/wave/sea ice models	None
Integration time step	50/3 seconds (3-stage Runge-Kutta method)
3. Surface boundary conditions	
Sea-surface temperature	Analyzed SST and sea-ice distribution
Land surface analysis	Climatological values of evaporability, roughness length and albedo Snow cover analysis from MSM
4. Lateral boundary conditions	
Model providing lateral boundary conditions	MSM
Lateral boundary condition update frequency	8 times/day 00 – 13-hour forecasts using the latest MSM information
5. Other details	
Soil scheme	Ground temperature prediction using an eight-layer ground model Evaporability prediction initialized using climatological values depending on location and season
Radiation	Short wave: two-stream with delta-Eddington approximation (every 15 minutes) Long wave: two-stream absorption approximation method (every 15 minutes)
Large-scale dynamics	Finite volume method with Arakawa-C-type staggered coordinates, horizontally explicit and vertically implicit time integration

	scheme, and combined third- and first-order upwind horizontal finite difference schemes in flux form with a limiter as proposed by Koren (1993) in advection treatment for monotonicity, time-splitting of vertical advection Fully compressible non-hydrostatic equations
Boundary layer	Mellor-Yamada-Nakanishi-Niino Level 3 scheme Similarity theory adopted for surface boundary layer
Convection	Convective initiation
Cloud/microphysics	Three-ice bulk cloud microphysics Time splitting of vertical advection for water substances Cloud water and cloud cover diagnosis using a partial condensation scheme
Orography	Mean orography smoothed to eliminate shortest-wave components
Horizontal diffusion	None
Gravity wave drag	None
6. Further information	
System documentation URL	http://www.jma.go.jp/jma/jma-eng/jma-center/nwp/nwp-top.htm

4.3.2.2 Research performed in this field

4.3.3 Operationally available NWP products

4.3.4 Operational techniques for application of NWP products

4.3.4.1 In operation

(1) Forecast guidance

Forecast guidance is utilized for the issuance of warnings, advisories, information and weather forecasts. The operational techniques routinely used to determine guidance from NWP model output are Kalman Filter (KF), Neural Network (NN), Multiple Linear Regression (MLR), Logistic Regression (LR), Diagnostic Methods (DM), and Lagged Average Forecast (LAF). These approaches are applied to grid-point values from the GSM, MSM and LFM in order to reduce systematic errors in NWP models and to extract useful information such as probabilities and categorical/diagnostic values. The specifications of weather forecast and aviation forecast guidance are listed in Tables 4.3.4-1 and 4.3.4-2, respectively.

Table 4.3.4-1 Weather forecast guidance specifications

Guidance based on GSM data is provided every 6 hours with forecast times between 3 and 84 hours every 3 hours. Guidance based on MSM data is provided every 3 hours with forecast times between 3 and 39 hours (51 hours for 00, 12 UTC initial) every 3 hours. Guidance based on LFM data is provided every hour with forecast times between 1 and 10 hours every hour.

Element	Details	Type	NWP	Statistical tool
Average precipitation	Mean precipitation amount over 3 hours (grid average)	Grid (20 * 20 km for GSM, 5 * 5 km	GSM, MSM	KF

Maximum precipitation	Maximum precipitation (within each grid square) over 1, 3, 12, 24, 48 and 72 hours (48 and 72 hours for GSM only)	for MSM)		NN (1, 3 hours), MLR (24 hours)
Probability of precipitation	Probability of precipitation totaling 1 mm or more over 6 hours			KF
Weather	Categorization (including sunshine duration and precipitation type)			NN (sunshine duration), DM (precipitation type)
Visibility	Minimum visibility			DM
Average precipitation	Mean precipitation amount over 1 hour (grid average)	Grid (5 * 5 km for LFM)	LFM	LAF
Maximum precipitation	Maximum precipitation over 1 hour (maximum value within each grid square)			
Maximum snowfall	Snowfall amount over 3, 6, 12 and 24 hours (maximum value within each grid square)	Grid (5 * 5 km)	GSM, MSM	DM + LR
Snowfall	Snowfall amount over 6, 12 and 24 hours	Point (323)		NN
Temperature	Maximum, minimum, time-series temperature	Point (928)		KF
Wind	Maximum, time-series wind speed/direction	Point (928)		KF
Humidity	Minimum humidity, time-series humidity	Point (154)		NN (minimum), KF (time series)
Probability of TS	Probability of thunderstorms	Grid (20 * 20 km)		LR

Table 4.3.4-2 Aviation forecast guidance specifications

Guidance based on the MSM is provided every 3 hours with forecast times between 1 and 39 hours (51 hours for 00 and 12 UTC initials) every hour. Guidance based on the LFM is provided every hour with forecast times between 1 and 10 hours every hour.

Element	Details	Type	NWP	Statistical tool
Visibility	Minimum and mean visibility	Point (91 airports)	MSM	KF
Probability of visibility	Probability of visibility less than 5,000 and 1,600 m			KF
Cloud	Cloud amount and height of lower 3 layers			NN
Probability of ceiling	Probability of ceiling below 600 and 1,000 ft			LR
Wind	Time-series, maximum wind speed/direction			KF
Gust	Gust speed/direction			KF
Probability of gusts	Probability of gusting			LR
Weather	Categorized weather			DM
Temperature	Maximum, minimum and time-series temperature			KF
Turbulence	Turbulence index	Grid (40 * 40 km and 28 layers for MSM, 10 * 10 km	GSM, MSM, LFM	LR

Icing	Icing index	and 45 layers for LFM)	GSM, MSM, LFM	DM
CB	CB cloud amount and CB top height		GSM, MSM, LFM	DM
Visibility	Minimum visibility		LFM	DM

(2) Hourly Analysis

Hourly Analysis involves three-dimensional evaluation of temperature and wind fields with a grid spacing of 5 km to provide real-time monitoring of weather conditions. The latest MSM forecast is used as the first guess, and observational information is added through data assimilation. The 3D-Var data assimilation method is adopted as the analysis technique, and the hourly product is made and distributed by 30 minutes past the hour. In July 2017, ASUCA data were adopted in a new system and a 3D-Var data assimilation system based on ASUCA (Aranami et al. 2015) was implemented, replacing the original one based on JMA-NHM (Saito et al. 2006, 2007) and JNoVA (Honda et al. 2005). The specifications of Hourly Analysis are listed in Table 4.3.4-3.

Table 4.3.4-3 Hourly Analysis specifications

Analysis time	Every hour on the hour
Analysis scheme	3D-Var
Data cut-off time	18 minutes past the hour
First guess	2, 3 or 4-hour forecast by MSM
Domain configuration	Japan and its surrounding area Lambert projection, 5 km at 60°N and 30°N, 721 × 577 Grid point (1, 1) is at the northwest corner of the domain. Grid point (489, 409) is at 140°E, 30°N.
Vertical coordinates	z-z^* hybrid
Vertical levels	48 levels up to 22 km
Analysis variables	Wind, temperature, surface wind and surface temperature
Observations (as of 31 December 2018)	AMeDAS, Wind Profiler, Weather Doppler radar (radial velocity), AIREP, AMDAR, and AMVs from Himawari-8
Post-processing	Surface filtering (followed by adjustment of the increment within the boundary layer)
Product distribution	By 30 minutes past the hour

4.3.4.2 Research performed in this field

(1) Forecast guidance

JMA is developing MEPS weather forecast guidance with variables of average precipitation, maximum precipitation, precipitation probability, visibility, maximum snowfall, snowfall, temperature, wind and TS probability. The elements of aviation forecast guidance are visibility, visibility probability, cloud, ceiling probability, wind, gusting, gusting probability, temperature, turbulence, icing and CB.

4.3.5 Ensemble Prediction System (EPS)

4.3.5.1 In operation

The Meso-scale Ensemble Prediction System (MEPS; specifications: Table 4.3.5-1) was introduced in June 2019 to provide uncertainty information for the MSM. It consists of 21 members, including one non-perturbed run, and is used to evaluate forecast uncertainty in consideration of initial and lateral boundary perturbations. Initial perturbations comprise a linear combination of global SVs (GSVs) based on the GSM and mesoscale SVs (MSVs) from JMA-NHM (Ono et al. 2011)), which have different spatial and temporal resolutions. Lateral boundary perturbations are supplied from linearly evolved GSVs (Ono 2017), ensuring consistency between initial and boundary conditions. The total energy norm (Ehrendorfer et al. 1999) is employed for perturbation growth metrics in SV definition. As the forecast model used in each ensemble member is exactly the same as the MSM, non-perturbed control forecast in MEPS is identical to MSM forecast.

Table 4.3.5-1 MEPS specifications

1. System	
System	Meso-scale Ensemble Prediction System
Date of implementation	27 June 2019
2. Configuration	
Domain	Japan and its surrounding area Lambert projection, 817 × 661 grid points
Horizontal resolution	5 km at 60 and 30°N (standard parallels)
Vertical levels	76
Model top	22 km
Forecast length	39 hours
Runs per day (times in UTC)	4 (00, 06, 12 and 18 UTC)
Members	One unperturbed control forecast and 20 perturbed ensemble members
Coupling with ocean/wave/sea ice models	None
Integration time step	100/3 seconds (3-stage Runge-Kutta method)
3. Initial conditions and perturbations	
Initial perturbation strategy	Singular vectors (SVs); linear combination of MSV40s, MSV80s and global SVs (GSVs)
Horizontal resolution of perturbations	MSV40: 40 km MSV80: 80 km GSV: Spectral triangular 63 (TL63), reduced Gaussian grid system, roughly equivalent to 2.8125 × 2.8125° (270 km) in latitude and longitude
Optimization time in forecast	MSV40: 6 hours MSV80: 15 hours GSV: 45 hours
Target area	MSV40: 125 – 145°E, 25 – 45°N MSV80: 125 – 145°E, 25 – 45°N GSV: 110 – 170°E, 15 – 50°N
Data assimilation for control analysis	4D-Var analysis with mixing ratios of cloud water, cloud ice, rain, snow and graupel derived from preceding forecasts in consideration of consistency with analysis field for relative humidity
Initial conditions for perturbed members	Perturbations added to control analysis in +/−pairs

4. Lateral boundary perturbations	
Lateral perturbation strategy	Based on integration of GSV (a large-scale component of initial perturbation) using the tangent linear model
5. Other model details	
	All ensemble members use exactly the same model as the MSM.

4.4 Nowcasting and Very-short-range Forecasting systems (0 – 15 hrs)

Since 1988, JMA has routinely operated a fully automated system of precipitation analysis and very short-range forecasting to monitor and forecast local severe weather conditions. In addition to these, JMA has issued Precipitation Nowcasts since June 2004, Thunder Nowcasts since May 2010 and Hazardous Wind Potential Nowcasts since May 2010. High-resolution Precipitation Nowcasts (JMA's latest nowcasting product) were introduced in August 2014. Extended Very-Short-Range Forecasts of precipitation (ExtVSRF) were introduced in June 2018. Snow Depth and Snowfall Amount Analysis were introduced in November 2019.

The products are listed below.

(1) High-resolution Precipitation Nowcasts (incorporating forecasts of 5-minute cumulative precipitation, 5-minute-interval precipitation intensity and error range estimation based on extrapolation and spatially three-dimensional forecasting covering the period up to 60 minutes ahead)
(2) Precipitation Nowcasts (incorporating forecasts of 10-minute cumulative precipitation and 5-minute-interval precipitation intensity based on extrapolation covering the period up to 60 minutes ahead)
(3) Thunder Nowcasts (incorporating forecasts of thunder and lightning activity based on lightning detection network system observation covering the period up to 60 minutes ahead)
(4) Hazardous Wind Potential Nowcasts (incorporating forecasts of the probability of hazardous wind conditions such as tornadoes covering the period up to 60 minutes ahead)
(5) Radar/Raingauge-Analyzed Precipitation (R/A)* (incorporating one-hour cumulative precipitation based on radar observation calibrated using raingauge measurements from JMA's Automated Meteorological Data Acquisition System (AMeDAS) and other available data such as those from rain gauges operated by local governments)
(6) Very-Short-Range Forecasts of precipitation (VSRFs) (incorporating forecasts of one-hour cumulative precipitation based on extrapolation and prediction by the MSM and LFM (see 4.3.2.1) and covering the period from one to six hours ahead)
(7) Extended VSRF (ExtVSRF) (incorporating forecasts of one-hour cumulative precipitation based on prediction and guidance from the MSM and LFM (see 4.3.2.1) and covering the period from 7 to 15 hours ahead)
(8) Snow Depth and Snowfall Amount Analysis (incorporating analysis of snow depth based on

estimates from a model simplifying temporal variations in snow properties modified using snow-depth gauge data from AMeDAS and analysis of snowfall amounts based on the increment between current and previous snow depths)

*Referred to before 15 November 2006, as *Radar-AMeDAS precipitation*.

4.4.1 Nowcasting system (0 – 1 hrs)

4.4.1.1 In operation

(1) High-resolution Precipitation Nowcasts

High-resolution precipitation nowcasts (HRPNs) provide five-minute-interval precipitation intensity and cumulative precipitation data up to an hour ahead. Initial precipitation intensity distribution is determined via three-dimensional analysis of storms using radar echo intensity, Doppler velocity, raingauge, surface and upper-air observation data.
Data on vertical atmospheric profiles are part of the input used for prediction generation. The initial values for such data are based on upper-air observation data, and are updated via comparison of cumulonimbus cloud profiles (echo top rising speed, ceiling height, lightning count and rainfall amount) between radar/radio-based observation and calculation using the Vertically One-dimensional Convective Model (VOCM). Thus, HRPNs are multi-observing-system-based nowcasting products beyond the scope of radar-based data with concentration on various observation data application technologies.

Two processes are adopted in HRPNs: (1) high-resolution three-dimensional prediction generated by extrapolating the three-dimensional distribution of water content and using VOCM data relating to notable regions of heavy rain, and (2) low-resolution three-dimensional prediction generated with a longer time step and reduced vertical calculation for areas outside high-resolution prediction regions. Data processing functions are designed for prediction using a dynamical estimation approach suitable for forecasting of rain phenomena that develop widely and rapidly based on a kinetic approach involving the extrapolation of phenomenon movement trends. Generation of data on convective cloud initiation triggered by three phenomena is also considered.
HRPN distribution data contain information on prediction uncertainty in the form of predictions regarding the magnitude of errors included in forecast rainfall. Knowledge of this uncertainty is considered useful in applications such as river water level prediction.
The specifications are summarized in Table 4.4.1-1.
HRPN are provided to local weather offices and the public to enable close monitoring of heavy-rain areas and support disaster prevention activities.

Table 4.4.1-1 High-resolution Precipitation Nowcast model specifications

Forecast process	• Kinetic: non-linear motion/intensity extrapolation • Dynamic: vertically one-dimensional convective model enabling calculation relating to raindrop generation, precipitation and evaporation • Convective Initiation: three triggers: (1) downflow caused by heavy rainfall, (2) temporal variation of surface temperature and water vapor, (3) intersection of arch-shaped thin echo
Movement vector	• Precipitation system, cell and rain intensity trend motion vectors estimated using cross-correlation pattern matching and discrete interpolation • Dual-Doppler wind
Time step	5 minutes (low-resolution three-dimensional prediction) 1 minute (high-resolution three-dimensional prediction) 1 second (vertically one-dimensional convective model)
Grid form	Cylindrical equidistant projection
Resolution and forecast time	Approx. 250 m over land and coasts 00 － 30 minutes ahead 1 km over land and coasts 35 － 60 minutes ahead 1 km from the coasts 00 － 60 minutes ahead
Number of grids	16,660,800 for distribution data, with up to 51,840,000 for internal calculation of high-resolution three-dimensional prediction
Initial	• Analyzed precipitation distribution determined from radar, raingauge and upper-air observation • Vertical atmospheric profiles based on radiosonde and cumulonimbus cloud features
Update interval	Every 5 minutes

(2) Precipitation Nowcasts

Precipitation Nowcasts predict 10-minute accumulated precipitation and 5-minute-interval precipitation intensity by extrapolation up to one hour ahead. Initial precipitation intensity distribution is derived from radar data obtained at 5-minute intervals, and is calibrated by raingauge observation. Using estimated movement vectors, these forecasts predict precipitation distribution on the basis of extrapolation. Calculation takes approximately three minutes. These processes are scheduled to be replaced with the smoothing applied for the output of High-resolution Precipitation Nowcasts. The specifications are summarized in Table 4.4.1-2.

Precipitation Nowcasts are provided to local weather offices and the public to help clarify precipitation transition and support disaster prevention activities.

Table 4.4.1-2 Precipitation Nowcast model specifications

Forecast process	Non-Linear motion/intensity extrapolation including the generation and lifecycle estimation of storm cells as well as orographic rainfall trend prediction
Movement vector	Precipitation system and/or cell motion estimated using the cross-correlation pattern matching and discrete interpolation
Time step	5 minutes
Grid form	Cylindrical equidistant projection
Resolution	Approx. 1 km
Number of grids	2,560 × 3,360
Initial	Calibrated radar echo intensities
Forecast time	60 minutes ahead, updated every 5 minutes

(3) Thunder Nowcasts

Thunder Nowcasts predict thunder and lightning activity up to an hour ahead. Initial activity distribution is derived from the lightning detection network system, radar data and Himawari-8/9 multiband observation conducted at 10-minute intervals. In consideration of estimated movement vectors, these forecasts predict activity distribution on the basis of extrapolation. Calculation takes approximately three minutes. The specifications are summarized in Table 4.4.1-3.

Thunder Nowcasts are provided to local weather offices and to the public. They are utilized to understand thundercloud transfer and to advise people to stay in or go to safe places in order to avoid lightning strikes.

Table 4.4.1-3 Thunder Nowcast model specifications

Forecast process	Extrapolation
Movement vector	As per the Precipitation Nowcast system
Grid form	Cylindrical equidistant projection
Resolution	Approx. 1 km
Number of grids	2,560 × 3,360
Initial	4-level activity of thunder and lightning based on the lightning detection network system, radar data and Himawari-8/9 high-frequency multiband observation
Forecast time	60 minutes ahead, updated every 10 minutes

(4) Hazardous Wind Potential Nowcasts

Hazardous Wind Potential Nowcasts predict the probability of hazardous wind conditions such as tornadoes up to one hour ahead. Initial probability distribution is established using radar measurements including Doppler radar data obtained at 10-minute intervals and severe weather parameters calculated from Numerical Weather Prediction. Using estimated movement vectors, these forecasts predict probability distribution on the basis of extrapolation. Calculation takes approximately three minutes. The specifications are summarized in Table 4.4.1-4.
Hazardous Wind Potential Nowcasts are provided to local weather offices and the public to clarify the transition of areas with high potential for hazardous winds and call attention to related hazardous conditions.

Table 4.4.1-4 Hazardous Wind Potential Nowcast model specifications

Forecast process	Extrapolation
Movement vector	As per the Precipitation Nowcast system
Grid form	Cylindrical equidistant projection
Resolution	Approx. 10 km
Number of grids	256 × 336
Initial	2-level presumed hazardous wind probabilities
Forecast time	60 minutes ahead, updated every 10 minutes

4.4.1.2 Research performed in this field

4.4.2 Models for Very-short-range Forecasting Systems (1 – 15 hrs)

4.4.2.1 In operation

(1) Radar/Raingauge-Analyzed Precipitation (R/A)

Radar data and raingauge precipitation data are analyzed every 30 minutes to create Radar/Raingauge Analyzed Precipitation (R/A) information with a resolution of 1 km. This involves the collection of radar echo intensity information from 46 weather radars operated by JMA and the Ministry of Land, Infrastructure, Transport and Tourism (MLIT) and precipitation data from more than 10,000 raingauges operated by JMA, MLIT and local governments.
Radar intensity readings are collected to create one-hour cumulative radar precipitation data, and are calibrated with one-hour cumulative raingauge precipitation data. R/A is a composite of all calibrated and cumulative radar precipitation data. The initial field for extrapolation forecasting is a composite of calibrated radar intensity data.
Dissemination of "Immediate R/A" information every 10 minutes was started in July 2017. This involves the collection of information from the same number of the weather radar and the less number of raingauges in contrast to the "Regular R/A".

(2) Very-Short-Range Forecasts of precipitation (VSRFs) (1 – 6 hrs)

The extrapolation forecast and precipitation forecast from the MSM and the LFM (see 4.3.2.1) are merged into the Very-Short-Range Forecast of precipitation (VSRFs). The merging weight of the MSM/LFM forecast is nearly zero for a one-hour forecast, and is gradually increased with forecast time to a value determined from the relative skill of MSM/LFM forecasts. The specifications of the extrapolation model are detailed in Table 4.4.2-1.

Table 4.4.2-1 Extrapolation model specifications used in VSRFs

Forecast process	Extrapolation
Physical process	Enhancement and dissipation
Movement vector	Precipitation system movement evaluated using the cross-correlation method
Time step	2 – 5 minutes
Grid form	Oblique conformal secant conical projection
Resolution	1 km
Number of grids	1,600 × 3,600
Initial	Calibrated radar echo intensities
Forecast time	Up to six hours from each initial time (every 10 minutes = 144 times/day)

Following on from the introduction of Immediate R/A data in 2017, JMA began providing Immediate VSRF data in March 2018. This information is issued every 10 minutes to support local weather offices that issue warnings for heavy precipitation, and is used for forecast calculation relating to

applied products such as the Soil Water Index and the Runoff Index.

(3) Extended Very-Short-Range Forecasts of precipitation (ExtVSRF) (7 – 15 hrs)

In June 2018, JMA launched its extended ExtVSRF forecast to support early judgement regarding the need for evacuation and other measures by clarifying the tendency of rainfall toward dawn when heavy rain falls in the evening. This forecast facilitates understanding of overall precipitation distribution as a trend, and was developed as a separate product from VSRF.
The forecast is derived from a combination of MSM precipitation amount forecasts, MSM Guidance for mean and maximum precipitation amounts and LFM Guidance for maximum precipitation amounts, and is not merged with EX6 data because the latter's precision from 7 to 15 hours ahead is significantly poorer than that produced by the combination of these guidance forecasts.
The latest available guidance forecasts for mean and maximum precipitation are divided into two groups and verified with current analysis R/A using the Fractions Skill Score (FSS). The forecast with the best score from each group is chosen and mixed with the weighted average.

Table 4.4.2-2 Forecast model specifications used in ExtVSRF

Forecast process	Combination of MSM precipitation amount forecasts, MSM Guidance for mean and maximum precipitation amounts and LFM Guidance for maximum precipitation amounts
Combination process	Verified with current analysis R/A using the Fractions Skill Score (FSS)
Grid form	Oblique conformal secant conical projection
Resolution	5 km
Number of grids	320 × 720
Forecast time	From seven to fifteen hours from each initial time (every hour = 24 times/day)

4.4.2.2 Research performed in this field

4.4.3 Snow Analysis System (0 hrs)

4.4.3.1 In operation

(1) Snow Depth and Snowfall Amount Analysis

The Snow Depth and Snowfall Amount Analysis products support mapping of snow depths and snowfall amounts, including for areas where snow depth observation is not conducted, and are issued every hour with a spatial resolution of 5 km.
Snow Depth Analysis is based on a model simplifying temporal variations in snow properties and is modified using AMeDAS snow gauge measurements. The model estimates snow depth based on fresh accumulation, melting and settling over time with R/A precipitation and precipitation, temperature and solar radiation from the LFM as inputs. Optimum interpolation is used to modify estimated snow depths.
Snowfall Amount Analysis is based on the increment between current and previous snow depths.

For values lower than previous data, a zero input is recorded.

Table 4.4.3-1 Snow Depth and Snowfall Amount Analysis specifications

Analysis process	Snow Depth Analysis is estimated using a model simplifying temporal variations in snow properties, modified using snow depth gauge measurements from AMeDAS. Snowfall Amount Analysis is based on the increment between current and previous snow depths.
Grid form	Cylindrical equidistant projection
Resolution	5 km
Number of grids	560 × 512
Analysis time	Every hour

4.4.3.2 Research performed in this field

4.5 Specialized numerical predictions

4.5.1 Assimilation of specific data, analysis and initialization (where applicable)

4.5.1.1 In operation

(1) Global Ocean Data Assimilation System

JMA's global ocean data assimilation system was upgraded in June 2015 to the MOVE/MRI.COM-G2 version (Toyoda et al. 2013) developed by its Meteorological Research Institute. Its specifications are shown in Table 4.5.1-1.

Table 4.5.1-1 Global Ocean Data Assimilation System specifications

Basic equations	Primitive equations with free surface
Independent variables	Lat-lon coordinates and σ-z hybrid vertical coordinates
Dependent variables	Zonal and meridional velocities, temperature, salinity and sea surface height
Analysis variables	Sea-surface and subsurface temperature and salinity
Numerical technique	Finite difference both in the horizontal and in the vertical
Grid size	1° (longitude) × 0.5° (latitude, smoothly decreasing to 0.3° toward the equator) grids
Vertical levels	52 levels with a bottom boundary layer
Integration domain	Global oceans
Forcing data	Heat, water and momentum fluxes calculated using data from the JRA-55 Reanalysis
Observational data	Sea-surface and subsurface temperature and salinity and sea surface height
Operational runs	Two kinds of run (final and early) with cut-off times of 33 days and 2 day, respectively, for ocean observation data

Outputs of MOVE/MRI.COM-G2 are used to monitor and diagnose tropical ocean status. Some figures based on MOVE/MRI.COM-G2 output are published in JMA's *Monthly Highlights on Climate System* and provided through the Tokyo Climate Center (TCC) website (http://ds.data.jma.go.jp/tcc/tcc/index.html). The data are also used as oceanic initial conditions for

JMA's coupled ocean-atmosphere model (JMA/MRI-CGCM2).

(2) High-resolution sea surface temperature analysis for global oceans and the western North Pacific

Objective analysis is conducted to produce high-resolution data on daily sea surface temperatures (SSTs) in global oceans on a 1/4° × 1/4° grid for ocean information services. These data are also used as boundary conditions for short- to medium-range NWP models and as observational data in the ocean data assimilation system for the North Pacific Ocean. SST data obtained from polar-orbiting satellites (AVHRRs on the NOAA series and Metop; Windsat on Coriolis; and AMSR2 on GCOM-W) are used together with in-situ SST observation data.

The HIMSST (High-resolution Merged Satellite and In-situ Data Sea Surface Temperature) analysis product, providing regional daily high-resolution (1/10 × 1/10°) analysis for the western North Pacific, was introduced in November 2016 with an analysis framework based on that of MGDSST along with components of smaller spatial and shorter temporal scales derived from Himawari-8 L3 SST (Kurihara et al. 2006). It has been used to provide boundary conditions for short-range NWP models, such as the Meso-Scale Model (MSM) and the Local Forecast Model (LFM), since March 2019.

The analysis data are available on the NEAR-GOOS Regional Real Time Database (https:// www.data.jma.go.jp/gmd/goos/data/database.html).

(3) Ocean wave analysis

A wave data assimilation system for JMA's operational wave model was put into operation in October 2012. The system is described below.

1) Wave data are not assimilated directly; the system refers to analysis wave heights of the JMA Objective Wave Analysis System (OWAS). The specifications are shown in Table 4.5.1-2. The key factor for rectification is the ratio of wave heights between model products and OWAS products.

2) In modification, windsea and swell parts are extracted and modified. Windsea spectra are modified based on the JONSWAP spectrum profile, and the peak frequency is determined in consideration of Toba's power law. For swell spectrum modification, the system rescales swell spectrum by the ratio of wave heights between model products and OWAS products. For details of the wave analysis system, refer to Kohno et al. (2012).

Table 4.5.1-2 JMA Objective Wave Analysis System (OWAS) specifications

Analysis scheme	Optimal interpolation
Data cut-off time	6 hours and 25 minutes for early-run analysis 12 hours for delayed analysis
First guess	6-hour forecast by the GWM
Analysis variables	Significant wave height
Grid size	0.5° (longitude) × 0.5° (latitude)
Integration domain	Global oceans
Observational data	BUOY, SHIP, Nowphas, GPS wave meter, JASON3, SARAL
Assimilation window	6 hours

4.5.1.2 Research performed in this field

4.5.2 Specific models

4.5.2.1 In operation

(1) Environmental emergency response system

JMA acts as a Regional Specialized Meteorological Center (RSMC) for Environmental Emergency Response in WMO Regional Association (RA) II, and is responsible for the preparation and dissemination of transport model products on exposure and surface contamination involving accidentally released radioactive materials. An operational tracer transport model is run at the request of National Meteorological Services in RA II and the International Atomic Energy Agency (IAEA) to offer RSMC support for environmental emergency response.

A Lagrangian method is adopted for the transport model, and large numbers of tracers are released at certain times and locations in line with pollutant emission information provided as part of related requests. Effects on three-dimensional advection and horizontal/vertical diffusion, dry and wet deposition and radioactive decay are computed from three-hourly outputs of the high-resolution global model (TL959L100). The standard products of the RSMC involve maps on trajectories, time-integrated low-level concentrations and total deposition up to 72 hours ahead.

As part of the CTBTO-WMO Backtracking Response System, JMA is responsible for providing atmospheric backtracking products to the Comprehensive Nuclear-Test-Ban Treaty Organization (CTBTO) in its role as a Regional Specialized Meteorological Center. JMA developed an atmospheric backtracking transport model and built up a response system that receives e-mail notifications from CTBTO, executes backtracking calculations and provides the resulting products in line with the procedure defined in WMO no. 485. JMA began operation of the backtracking system in December 2009. Backtracking over a period up to 50 days can be provided on an operational basis.

(2) Ocean-wave forecasting models

JMA operates four numerical wave models: the Global Wave Model (GWM), the Coastal Wave Model (CWM), the Wave Ensemble System (WENS), and the Shallow-water Wave Model (SWM). The GWM, CWM and WENS are based on MRI-III, which was developed at JMA's Meteorological Research Institute (MRI), and a major update was made to the current version in May 2007. The WENS has been operational since June 2016. The specifications of the models are given in Table 4.5.2.1 (2)-1.

JMA began calculating wave components (windsea and swell) for the GWM and CWM on 20 July 2016. Since the upgrade of JMA's supercomputer system on 5 June 2018, the forecast lengths of the

GWM and CWM initialized at 00, 06 and 18 UTC have been extended from 84 to 132 hours, and the model run frequency of the WENS has been increased from once to twice a day.

The SWM is based on the WAM, which was modified at the National Institute for Land and Infrastructure Management of MLIT and put into operation under a cooperative framework with MLIT's Water and Disaster Management Bureau. The model is applied to 22 sea areas along the coast of Japan. The models' specifications are given in Table 4.5.2.1 (2)-2.

Table 4.5.2.1 (2)-1 Ocean-wave prediction model specifications

Model name	Global Wave Model	Coastal Wave Model	Wave Ensemble System
Model type	Spectral model (third-generation wave model)		
Date of implementation	May 2007	May 2007	June 2016
Grid form	Equal latitude-longitude grid on spherical coordinates		
Grid interval	0.5° × 0.5° (55 km)	0.05° × 0.05° (5 km)	1.25° × 1.25° (140 km)
Calculation area	Global 75°N – 75°S	Coastal Sea of Japan 50°N – 20°N, 120°E – 150°E	Global 75°N – 75°S
Grids	720 × 301	601 × 601	288 × 121
Spectral components	900 (25 frequencies and 36 directions) Frequency: 0.0375 – 0.3 Hz; logarithmically divided direction: 10° intervals		
Forecast cycle	4 times a day (every 6 hours)		Twice a day (every 12 hours)
Forecast length (12 UTC) (00/06/18 UTC)	 264 hours 132 hours	 132 hours 132 hours	 264 hours
Forecast time interval	Every 3 hours	Every 3 hours	Every 6 hours
Time step	Advection term: 10 minutes Source term: 30 minutes	Advection term: 1 minute Source term: 3 minutes	Advection term: 30 minutes Source term: 60 minutes
Assimilation	Wave height analyzed using the Objective Wave Analysis System Initial conditions modified using analysis wave height		
Surface forcing	Global Spectral Model (GSM) (20 km grid) Winds inside typhoons modified using ideal gradient wind values (– 72 hours)		Global Ensemble Prediction System (GEPS) 27 members
Lateral boundary	Sea ice: analysis area regarded as land	Sea ice: analysis area regarded as land GWM prediction used for boundary spectra	Sea ice: analysis area regarded as land
Shallow-water effects	Refraction and bottom friction	Refraction and bottom friction	No
Product	Significant wave height, wave period and mean wave direction Wave components (windsea and two swells) also calculated		

Table 4.5.2.1 (2)-2 Shallow-water wave model specifications

Model name	Shallow-water Wave Model
Model type	Spectral model (third-generation wave model)

Grid interval	1' × 1' (1.7 km)		
Spectral components	1,260 (35 frequencies from 0.0418 to 1.1 Hz and 36 directions)		
Grid form	Equal latitude-longitude grid on spherical coordinates		
Areas	Domain name	Grid size	Integration domain
	Tokyo Bay	37 × 43	35.05°N – 35.75°N 139.55°E – 140.15°E
	Ise Bay	61 × 43	34.35°N – 35.05°N 136.45°E – 137.45°E
	Harima-Nada Osaka Bay	79 × 49	34.05°N – 34.85°N 134.15°E – 135.45°E
	Ariake Sea Shiranui Sea	43 × 73	32.05°N – 33.25°N 130.05°E – 130.75°E
	Off Niigata	55 × 37	37.80°N – 38.40°N 138.35°E – 139.25°E
	Sendai Bay	37 × 43	37.75°N – 38.45°N 140.90°E – 141.50°E
	Off Tomakomai	121 × 43	42.00°N – 42.70°N 141.00°E – 143.00°E
	Suo-Nada Iyo-Nada Aki-Nada	109 × 67	33.30°N – 34.40°N 131.00°E – 132.80°E
	Hiuchi-Nada	103 × 73	33.60°N – 34.80°N 132.60°E – 134.30°E
	Off Shimane	67 × 31	35.25°N – 35.75°N 132.55°E – 133.65°E
	Ishikari Bay	49 × 43	43.10°N – 43.80°N 140.70°E – 141.50°E
	Off Ishikawa	49 × 67	36.20°N – 37.30°N 136.00°E – 136.80°E
	Off Nemuro	85 × 49	43.20°N – 44.00°N 145.00°E – 146.40°E
	Off Miyazaki	31 × 73	31.50°N – 32.70°N 131.30°E – 131.80°E
	Tsugaru Strait	61 × 67	40.75°N – 41.85°N 140.35°E – 141.35°E
	Off Ibaraki Off Boso	49 × 103	35.00°N – 36.70°N 140.20°E – 141.00°E
	Genkai-Nada	85 × 43	33.40°N – 34.10°N, 129.55°E – 130.95°E
Forecast cycle	4 times a day (every 6 hours) at initial times of 03, 09, 15 and 21 UTC		
Forecast length	39 hours		
Forecast step interval	Hourly		
Integration time step	Advection term: 1 minute Source term: 1 minute		
Assimilation	No (hindcast)		
Surface forcing	Meso-Scale Model (MSM)		
	Bogus gradient winds (for typhoons in the western North Pacific)		
Lateral boundary	Sea ice: analysis area regarded as land CWM prediction used for boundary spectra		
Shallow-water effects	Refraction and bottom friction		
Product	Significant wave height, wave period and mean wave direction		

Wave model products are adopted by various domestic users (such as governmental organizations and private weather companies) via the Japan Meteorological Business Support Center (JMBSC), whereas SWM products are only used within JMA and MLIT's Regional Development Bureaus.

GWM products are available within JMA's WMO Information System for National Meteorological and Hydrological Services (NMHSs), and are also disseminated to several countries via GTS.

(3) Storm surge models

JMA operates two storm surge models. One is used to predict storm surges in coastal areas of Japan using sea-surface wind and pressure fields inferred by the MSM. In the case of tropical cyclones (TCs), storm surges for six scenarios are predicted in consideration of TC track forecast errors. In addition to the MSM, TC bogus data corresponding to five tracks (center, faster, slower and rightmost/leftmost of the TC track forecast) are used for each scenario. Data on astronomical tides are required for the prediction of storm tides (i.e., the sum of storm surges and astronomical tides). Astronomical tides are estimated using an ocean tide model and added linearly to storm surges. The model's specifications are given in Table 4.5.2.1 (3)-1.

Table 4.5.2.1 (3)-1 Storm-surge model (Japan region) specifications

Basic equations	Two-dimensional shallow-water equations
Numerical technique	Explicit finite difference method
Integration domain	Coastal areas of Japan (117.4°E – 150.0°E, 20.0°N – 50.0°N)
Grid	Adaptive Mesh Refinement (AMR) method 45 seconds (longitude gradually doubling to 12 minutes toward offshore areas) × 30 seconds (latitude gradually doubling to 8 minutes toward offshore areas)
Boundary conditions	Modified radiation condition at open boundaries and zero normal flows at coastal boundaries
Forecast time	39 hours
Forcing data	Meso-Scale Model (MSM)
	Bogus data for TCs around Japan
Astronomical tides	Ocean tide model (Egbert and Erofeeva 2002) and data assimilation of harmonic constants at tide stations using the ensemble transform Kalman filter (ETKF)

As part of JMA's contribution to the Storm Surge Watch Scheme (a WMO framework supporting member countries in the issuance of storm surge warnings), the Agency developed a storm surge model for the Asian region in 2010 in collaboration with Typhoon Committee Members who provided tidal observation and sea bathymetry data. The model uses the GSM for meteorological forcing. For TCs, in addition to the GSM and TC bogus, multi-scenario predictions are calculated for five selected scenarios from GEPS data. The resulting storm surge prediction information is provided to Typhoon Committee Members via JMA's Numerical Typhoon Prediction website. The model's specifications are given in Table 4.5.2.1 (3)-2.

Table 4.5.2.1 (3)-2 Storm-surge model (Asian region) specifications

Basic equations	Two-dimensional linear shallow-water equations

Numerical technique	Explicit finite difference method
Integration domain	Coastal areas of Asia (95.0°E – 160.0°E, 0.0°N – 46.0°N)
Grid	2 minutes × 2 minutes
Boundary conditions	Modified radiation condition at open boundaries and zero normal flows at coastal boundaries
Forecast time	72 hours
Forcing data	Global Spectral Model (GSM), Global EPS (GEPS)
	Bogus data for TCs (center)
Astronomical tides	Not included

(4) Ocean data assimilation system for the North Pacific Ocean

A 3D-Var ocean data assimilation system for the North Pacific is operated to represent ocean characteristics such as the Kuroshio path variation in the mid/high latitudes of the North Pacific with the specifications shown in Table 4.5.2.1 (4)-1. Data on ocean currents and several layers of subsurface water temperatures (products of this system) are available on the NEAR-GOOS Regional Real Time Database (https://www.data.jma.go.jp/gmd/goos/data/database.html).

Table 4.5.2.1 (4)-1 Specifications of the 3D-Var ocean data assimilation system for the North Pacific Ocean

Basic equations	Primitive equations with free surface
Independent variables	Lat-lon coordinates and σ-z hybrid vertical coordinates
Dependent variables	Zonal/meridional velocities, temperature, salinity and sea surface height
Analysis variables	Sea-surface/subsurface temperature and salinity
Numerical technique	Finite difference both in the horizontal and in the vertical
Grid size	(1) Western North Pacific model 0.1° longitude × 0.1° latitude in the seas off Japan, decreasing to 0.166° toward the northern and eastern boundaries (2) North Pacific model 0.5° longitude × 0.5° latitude
Vertical levels	54
Integration domain	(1) Western North Pacific model From 15°N to 65°N between 115°E and 160°W (2) North Pacific model From 15°S to 65°N between 100°E and 75°W
Forcing data	Heat, water and momentum fluxes from the Japanese 55-year Reanalysis (JRA-55) and from the control run of Global Ensemble Prediction System (GEPS)
Assimilation scheme	3D-Var with 5-day windows
Observational data (as of 31 December 2019)	Sea-surface and subsurface temperature/salinity, sea surface height (Jason-3, Cryosat-2, Saral), sea ice concentration
Operational runs	10-day assimilation and 30-day prediction are implemented every day

(5) Sea-ice forecasting model

JMA issues information on the state of sea ice in the seas off Japan. A numerical sea-ice model has been run to predict sea ice distribution and thickness in the seas off Hokkaido (mainly in the southern part of the Sea of Okhotsk) twice a week in winter since December 1990 (see Table 4.5.2.1

(5)-1).

Table 4.5.2.1 (5)-1 Numerical sea-ice prediction model specifications

Dynamical processes	Viscous-plastic model (MMD/JMA 1993) – considering wind and seawater stress on sea ice, Coriolis force, force from the sea surface gradient and internal force
Physical processes	Heat exchange between sea ice, the atmosphere and seawater
Dependent variables	Concentration and thickness
Grid size and time step	12.5 km and 6 hours
Integration domain	Seas around Hokkaido
Initial time and forecast time	168 hours from 00 UTC (twice a week)
Initial condition	Concentration analysis derived from Himawari-8/9, NOAA and Metop satellite imagery; thickness estimated by hindcasting

Grid-point values of the numerical sea-ice model are disseminated to domestic users. Sea ice conditions for the coming seven days as predicted by the model are broadcast by radio facsimile (JMH) twice a week.

(6) Marine pollution transport model

JMA operates the numerical marine-pollution transport model in the event of marine-pollution accidents. Its specifications are shown in Table 4.5.2.1 (6)-1. The ocean currents used for the model's input data are derived from the results of the ocean data assimilation system for the North Pacific Ocean.

Table 4.5.2.1 (6)-1 Marine pollution transport model specifications

Area	Western North Pacific
Grid size	2 – 30 km (variable)
Model type	3-dimensional parcel model
Processes	Advection caused by ocean currents, sea surface winds and ocean waves Turbulent diffusion Chemical processes (evaporation, emulsification)

(7) Aeolian dust prediction model

JMA has operated a prediction model since January 2004 to forecast Aeolian dust distribution. The model was updated to a new version based on an Earth-system model (MRI-ESM1; Yukimoto et al. 2011; Yukimoto et al. 2012) for global climate change research in November 2014, and the horizontal resolution was enhanced from TL159 to TL479 in February 2017. The model consists of an atmospheric general circulation model (AGCM) called MRI-AGCM3 and a global aerosol model called MASINGAR mk-2, which are linked with a coupler library called Scup (Yoshimura and Yukimoto 2008). The dust emission flux calculation method was updated to encompass the scheme of Tanaka and Chiba (2005) in November 2014. The model's specifications are given in Table 4.5.2.1 (7)-1.

Table 4.5.2.1 (7)-1 Aeolian dust prediction model specifications

Basic equations	Eulerian model coupled with the Global Spectral Model
Numerical technique	3D semi-Lagrangian transport and dust emission calculation from surface meteorology
Integration domain	Global
Grid size	TL479 (0.375°)
Vertical levels	40 (surface – 0.4 hPa)
Initial time and forecast time	96 hours from 12 UTC (once a day)
Boundary conditions	Similar to those of the Global Spectral Model
Forcing data (nudging)	Global Analysis (GA) and Global Spectral Model (GSM) forecasts
	Sea surface temperature (MGDSST)

(8) Ultraviolet (UV) index prediction system

JMA has operated a UV index prediction system since May 2005. The UV index is calculated using a chemical transport model (CTM) that predicts the global distribution of ozone and a radiative transfer model. In October 2014, the ozone chemistry model was updated to a new version of the chemistry-climate model (MRI-CCM2; Deushi and Shibata 2011), which is part of MRI-ESM1, and its horizontal resolution was enhanced from T42 to T106 (see Table 4.5.2.1 (8)-1 for model specifications).

The radiative transfer model (Aoki et al. 2002) calculates the UV index in the area from 122°E to 149°E and from 24°N to 46°N with a grid resolution of 0.25° × 0.20°. The Look-Up Table (LUT) method is adopted in consideration of the computational cost involved. The basic parameters of LUT are the solar zenith angle and total ozone predicted using the CTM. The clear sky UV index is corrected for distance from the sun to the earth, aerosols (climatology), altitude and surface albedo (climatology). The forecast UV index is corrected for categorized weather forecasts in addition to the above-mentioned factors. The specifications of the radiative transfer model for the UV index are given in Table 4.5.2.1 (8)-2.

Table 4.5.2.1 (8)-1 Specifications of the chemical transport model in the UV index prediction system

Basic equations	Eulerian model coupled with the Global Spectral Model
Numerical technique	3D semi-Lagrangian transport and chemical reaction
Integration domain	Global
Grid size	T106 (1.125°)
Vertical levels	64 (surface – 0.01 hPa)
Initial time and forecast time	48 hours from 12 UTC (once a day)
Boundary conditions	Similar to those of the Global Spectral Model
Forcing data (nudging)	Global analysis (GA) and Global Spectral Model (GSM) forecasts
Observational data	Column ozone from OMPS/NOAA

Table 4.5.2.1 (8)-2 Specifications of the radiative transfer model in the UV index prediction system

Basic equations	Radiative transfer equations for multiple scattering and

	absorption by atmospheric molecules and aerosols
Numerical technique	Doubling and adding method
Spectral region and resolution	280 – 400 nm and 0.5 nm

(9) Regional chemical transport model for photochemical oxidants

JMA provides prefectural governments with photochemical smog bulletins as a basis for related advisories. The bulletins are produced by numerical model prediction of tropospheric photochemical oxidant distribution and a statistical guidance derived from model outputs associated with past events.

Since March 2015, numerical model prediction of photochemical oxidants has been carried out using a regional chemical transport model with finer spatial resolution (NHM-Chem; Kajino et al. 2019) driven with meteorological fields predicted using an offline non-hydrostatic atmospheric model (JMA-NHM). The related lateral and upper boundary conditions for chemical species are given by MRI-CCM2 as described in 4.5.2.1 (8).

Since March 2017, surface ozone concentration data have been assimilated in photochemical oxidant prediction. The specifications of the regional chemical transport model are given in Table 4.5.2.1 (9)-1.

The NHM-Chem source code is available subject to a license agreement with the Japan Meteorological Agency. Further resources, including a user's manual and analysis tools, can be provided upon request to the Meteorological Research Institute.

Table 4.5.2.1 (9)-1 Specifications of the regional chemical transport model for photochemical oxidants

Model type	3-dimensional Eulerian chemical transport model
Area	East Asia
Grid size	20 km
Vertical layers	18 (surface – 10 km)
Forecast time	66 hours (initial time 18 UTC)
Emission inventories	REAS1.1, GFED3 and MEGAN2
Meteorological fields	JMA-NHM output constrained and initialized using Global Analysis (GA) and Global Spectral Model (GSM) forecasts
Observational data	Surface O_3 concentration of Atmospheric Environmental Regional Observation System (AEROS**)

** Available from http://soramame.taiki.go.jp/

(10) Mesoscale air pollution transport model

JMA also issues very-short-term photochemical smog bulletins on days when high oxidant concentration is expected. The bulletins provide an outlook for photochemical smog based on statistical guidance for oxidant concentration using data on weather elements and pollutant observation data as input. In addition to this statistical guidance, a mesoscale atmospheric transport model (Takano et al. 2007) is applied to very-short-range forecasting of oxidant concentrations with

a grid interval of 10 km, with MSM output used to calculate the transport of highly concentrated pollutant masses in the air. Based on the oxidant forecast from the atmospheric transport model with an initial time of 03 UTC (noon in Japan), photochemical smog bulletins show hourly potential for afternoon smog in the northern part of the Kyushu region and the Kanto region, where the Tokyo metropolitan area is located.

(11) Regional Atmospheric Transport Model (RATM) for volcanic ash

JMA introduced the Volcanic Ash Fall Forecast (VAFF) based on the Regional Atmospheric Transport Model (RATM) in March 2008 (Shimbori et al. 2009) and updated it in spring 2015 (Hasegawa et al. 2015). Three types of forecasts are sequentially provided: VAFFs (Scheduled) are issued periodically based on an assumed eruption for active volcanoes, VAFFs (Preliminary) are brief forecasts issued within 5 － 10 minutes of an actual eruption, and VAFFs (Detailed) are more accurate forecasts issued within 20 － 30 minutes of an actual eruption. The updated VAFFs provide information on expected ash/lapilli fall areas and/or amounts based on the RATM with LFM or MSM outputs. The specifications of RATM are given in Table 4.5.2.1 (11)-1.

Table 4.5.2.1 (11)-1 Specifications of RATM for volcanic ash

Model type	Lagrangian description
Number of tracer particles	100,000 (Scheduled, Preliminary) 250,000 (Detailed)
Time step	1 minute (Preliminary) 3 minutes (Scheduled, Detailed)
Forecast time	18 hours from the time of assumed eruption (Scheduled) 1 hour from the time of eruption (Preliminary) 6 hours from the time of eruption (Detailed)
Initial condition	Eruption column based on observational reports including eruption time and plume height, and continuance of volcanic-ash emissions
Meteorological field	Local Forecast Model (LFM) or Meso-Scale Model (MSM)
Processes	3D advection, horizontal and vertical diffusion, volcanic-ash fallout, dry deposition and washout

(12) Global Atmospheric Transport Model (GATM) for volcanic ash

Since 1997, JMA has been providing information on volcanic ash clouds to airlines, civil aviation authorities and related organizations in its role as the Volcanic Ash Advisory Centre (VAAC) Tokyo. JMA introduced the Global Atmospheric Transport Model (GATM) in December 2013 as an 18-hour prediction of areas where ash clouds are expected in the area of responsibility as a result of volcanic eruptions. The forecast is normally updated every six hours (00, 06, 12 and 18 UTC) for as long as ash clouds are identified in satellite imagery. The specifications of the GATM are given in Table 4.5.2.1 (12)-1.

Table 4.5.2.1 (12)-1 Specifications of GATM for volcanic ash

Model type	Lagrangian description

Number of tracer particles	40,000
Time step	10 minutes
Forecast coverage	18 hours from the time of satellite observation
Initial condition	Location of volcanic ash particles based on the area and maximum altitude of volcanic ash cloud observed by satellite
Meteorological field	Global Spectral Model (GSM)
Processes	3D advection, (horizontal and vertical diffusion,) volcanic-ash fallout, dry deposition and washout

4.5.2.2 Research performed in this field

(1) Storm surge model

A new storm surge model that solves governing equations using the finite volume method on an unstructured grid is currently being developed. The use of such a grid allows grid-size flexibility, which is expected to enable improvements in forecast accuracy and computational efficiency compared to current models. The new model will be incorporated into both storm surge prediction systems.

(2) Sea-ice forecasting model

JMA plans to replace the current sea ice model (see 4.5.2.1 (5)) with the new one included in a coastal ocean analysis/forecasting system (MOVE/MRI.COM-JPN) (see 6.1.2 (23)). Sea ice data from MOVE/MRI.COM-JPN are currently being verified for operational use.

(3) Aeolian dust prediction model

Previous aerosol reanalysis research has included a development version of the Aeolian dust forecasting model and 2D-Var data assimilation with the NRL-UND MODIS L3 AOT product (Yumimoto et al. 2017). The reanalysis products are available from the authors upon request. Other research on determining aerosol properties from satellite data combined with assimilated aerosol forecasting is conducted in conjunction with JAXA/EORC, and a data assimilation system involving the implementation of a local ensemble transform Kalman filter (LETKF) (Sekiyama et al. 2010, 2016; Yumimoto et al. 2016 a, 2016 b) for application of satellite observation data is in the research phase.

(4) UV index prediction system

Research is being performed on a data assimilation system for stratospheric ozone involving the use of satellite data with 2D-Var data toward operational application.

(5) Regional chemical transport model

A nudging technique for surface ozone data assimilation has been applied to the regional chemical transport model. JMA is currently evaluating this application for the photochemical oxidant information advisory. Research toward the implementation of 2D-Var data assimilation is also ongoing toward improved prediction for photochemical oxidants and aerosols.

(6) Volcanic ash concentration forecast

Despite the importance of volcanic ash concentration forecasting in the world of aviation, no method for such prediction has yet been developed. JMA is currently evaluating a forecast method involving calculation with weight coefficients for individual particles, based on the comparison of actual results with observation data for past eruptions.

(7) Improvement of initial conditions for volcanic ash forecasts

JMA is currently developing a method to improve data on the initial distribution of volcanic ash for numerical prediction using estimation of ash cloud thickness.

(8) Ocean data assimilation system for the North Pacific Ocean

A 4D-Var ocean data assimilation system has been quasi-operational since March 2016 with the same integration domain, grid size and vertical levels as those of the 3D-Var system (Table 4.5.2.1 (4)-1). With the Global Spectral Model (GSM) used for forcing data, 10-day assimilation and 11-day prediction are implemented on a daily basis. This 4D-Var system is part of a prototype for the future operational analysis/forecasting system (MOVE/MRI.COM-JPN) being developed by JMA's Meteorological Research Institute (see 6.1.2). Its output is used as reference for the development of the next operational system.

4.5.3 Specific products operationally available

(1) Storm surge prediction products

Time series representations of predicted storm tides/astronomical tides and forecast time on predicted highest tides for the coastal area in Japan are disseminated to local meteorological observatories. This information is used as a major basis for issuing storm surge advisories and warnings. For the area of responsibility of the RSMC Tokyo - Typhoon Center, horizontal maps and time-series charts of storm surge predictions are provided to Typhoon Committee members via JMA's

Numerical Typhoon Prediction website.

(2) Ocean wave forecast charts

Products from the ocean wave models shown in Table 4.2.3-1 are provided via JMA's radio facsimile broadcast (JMH) service. In addition to basic wave information such as significant wave height and wave direction, information on rough sea areas, which may be challenging for navigation, has been included in Wave Forecast Charts since March 2017. The information indicates areas of crossing waves and rough waves against currents, which make seas complex, high and chaotic.

(3) Aeolian dust products operationally available

Predicted distributions of surface concentration and the total amount of Aeolian dust in eastern Asia are provided online (https://www.data.jma.go.jp/gmd/env/kosa/fcst/en/) once a day.

(4) UV index products operationally available

Distributions and time series representations of predicted UV index information are provided online (https://www.data.jma.go.jp/gmd/env/uvindex/en/) twice a day.

4.6 Extended-range forecasts (ERFs) *(10 – 30 days)*

4.6.1 Models

4.6.1.1 In operation

The Global EPS (GEPS) referred to in 4.2.5.1 seamlessly covers medium- to extended-range forecasting. The GEPS forecast range is extended from 11 to 18 days for initial times every day and to 34 days for initial times on Tuesday and Wednesday. JMA's 18-day forecasts support the issuance of early warning information on extreme weather, and 34-day forecasts support one-month forecasting.

The specifications of the GEPS for forecasts longer than 11 days are shown in Table 4.6.1.1-1. The numerical prediction model applied for this system is a low-resolution version (TL479 up to 18 days and TL319 thereafter) of the GSM. The physical schemes and perturbation methods for forecasts longer than 11 days are shared with those for forecasts up to 11 days, while the prescription of sea ice and the combination of ensemble members are unique. Sea ice concentration for forecasts longer than 14 days is prescribed by adjusting the previous day's distribution so that initial sea ice extent anomalies in each hemisphere persist. In addition, because the ensemble size for each initial time is reduced from 27 to 13 for forecasts longer than 11 days due to limited computer resources, JMA

adopts the Lagged Average Forecast (LAF) method composed of four 12-hour-interval forecasts for periods exceeding 11 days to ensure a significant ensemble member size and appropriate consideration of forecast uncertainty. Specifically, 50 members (13 at 00 and 12 UTC over the previous two days) are used for the issuance of early warning information on extreme weather on Thursday/Monday and one-month forecasts on Thursday.

Table 4.6.1.1-1 Global EPS specifications for forecasts longer than 11 days

Atmospheric model	GSM1603E
Integration domain	Global
Horizontal resolution	Spectral triangular 479 (TL479), reduced Gaussian grid system, roughly equivalent to 0.375 × 0.375° (40 km) in latitude and longitude for forecasts up to 18 days Spectral triangular 319 (TL319), reduced Gaussian grid system, roughly equivalent to 0.5625 × 0.5625° (55 km) in latitude and longitude for forecasts longer than 18 days
Vertical levels (model top)	100 stretched sigma pressure hybrid levels (0.01 hPa)
Forecast time	18 days for initial times every day 34 days for initial times on Tuesday and Wednesday
Ensemble size	50 members (13 at 00 and 12 UTC over the previous two days)

4.6.1.2 Reanalysis project

In March 2013, JMA completed the second Japanese global reanalysis, known formally as JRA-55 (Kobayashi et al. 2015) and informally as JRA Go! Go! (as "go" is the Japanese word for "five"), to provide a comprehensive atmospheric dataset suitable for the study of climate change and multi-decadal variability. The data cover a period of 55 years extending back to 1958 when regular radiosonde observations became operational on a global basis. The data assimilation system for JRA-55 is based on the TL319 version of JMA's operational data assimilation system as of December 2009, which has been extensively improved since the JRA-25 dataset was produced (Onogi et al. 2007). JRA-55 is the first global atmospheric reanalysis in which four-dimensional variational assimilation (4D-Var) was applied to the last half century including the pre-satellite era. Its production also involved the use of numerous newly available and improved past observations. The resulting reanalysis products are considerably better than those based on the JRA-25 dataset. Two major problems with JRA-25 were a lower-stratosphere cold bias, which has now been reduced, and a dry bias in the Amazon basin, which has been mitigated. The temporal consistency of temperature analysis has also been considerably improved. JMA continues the production of JRA-55 dataset on a near-real-time basis with the data assimilation system used for this dataset.

4.6.2 Operationally available NWP model and EPS ERF products

A model systematic bias was estimated as an average forecast error calculated from hindcast experiments for the years from 1981 to 2010. The bias is removed from forecast fields, and grid-point

values are processed to produce several forecast materials such as ensemble means and spreads.

Gridded data products for one-month forecast are provided via the Tokyo Climate Center (TCC) website (http://ds.data.jma.go.jp/tcc/tcc/index.html). Details of these products are shown in Table 4.6.2-1, and map products provided via the TCC are shown in Table 4.6.2-2.

Table 4.6.2-1 Gridded data products (GRIB2) for one-month forecasts provided via the TCC website

Details		Level (hPa)	Area	Base time & forecast times
Ensemble mean value of forecast members	Sea level pressure* and its anomaly	-	Global 2.5˚ × 2.5˚	Base time: 00 UTC of Wednesday Forecast time: 2, 3, 4…,31,32 days from base time
	Rainfall amount and its anomaly	-		
	Temperature and its anomaly	Surf, 850, 700		
	Relative humidity	850		
	Geopotential height and its anomaly	500, 100		
	Wind (u, v)	850, 200		
	Stream function and its anomaly	850, 200		
	Velocity potential and its anomaly	200		
Individual ensemble members	Sea level pressure*	-		Base time: 00 UTC of Tuesday and Wednesday Forecast time: 0, 1, 2,..., 31, 32 days from base time
	Rainfall amount	-		
	Temperature*	Surf, 1000, 850, 700, 500, 300, 200, 100		
	Relative humidity	1000, 850, 700, 500, 300		
	Geopotential height*	1000, 850, 700, 500, 300, 200, 100		
	Wind (u,v)	1000, 850, 700, 500, 300, 200, 100		
	Stream function	850, 200		
	Velocity potential	200		

* Geopotential height, sea level pressure and temperature are calibrated by subtracting the systematic error from the direct model output.

Table 4.6.2-2 Map products for one-month forecasts provided via the TCC website

	Forecast time	Parameter
Ensemble mean	Averages of days 3 – 9, 10 – 16, 17 – 30, 3 – 30	Geopotential height at 500 hPa and its anomaly Temperature at 850 hPa and its anomaly Sea level pressure and its anomaly Stream function at 200 hPa and its anomaly Stream function at 850 hPa and its anomaly Velocity potential at 200 hPa and its anomaly Precipitation and its anomaly Temperature at 2 m and its anomaly Sea surface temperature (prescribed)

4.7 Long range forecasts (LRF) (30 days up to two years)

4.7.1 Models

4.7.1.1 In operation

JMA operates its Seasonal Ensemble Prediction System (Seasonal EPS; JMA/MRI-CPS2) using an atmosphere-ocean coupled model (JMA/MRI-CGCM2) for three-month, warm/cold season and El Niño outlooks. The current system was upgraded in June 2015. The 51-member ensemble is used for the three-month forecast issued every month and for the warm/cold season forecasts issued five times a year (in February, March, April, September and October). The El Niño outlook is also issued based on the same model results.

The JMA/MRI-CGCM2 was developed by the Meteorological Research Institute and the Climate Prediction Division of JMA. Its specifications are shown in Table 4.7.1-1. Atmospheric and land surface initial conditions are taken from JRA-55 data (Kobayashi et al. 2015; 4.6.1.2), while oceanic and sea ice initial conditions are taken from MOVE/MRI-COM-G2 (4.5.1.1 (1)). The EPS adopts a combination of the LAF method and the initial perturbation method described below. Thirteen-member ensemble predictions are made every five days, and atmospheric initial perturbations for each initial date are obtained using the BGM method. Oceanic initial perturbations are obtained with MOVE/MRI.COM-G2 forced by the surface heat and momentum fluxes of atmospheric initial perturbation fields using the BGM method.

Table 4.7.1-1 Seasonal EPS specifications

Model	JMA/MRI-CGCM2 An atmosphere-ocean coupled model rather than a Tier-2 system	
Atmospheric model	Model type	GSM1011C
	Horizontal resolution	Global TL159 reduced Gaussian grid system roughly equivalent to 1.125 × 1.125° (110 km) in latitude and longitude
	Vertical levels (model top)	60 levels (0.1 hPa)
Oceanic model	Model type	MRI.COM v3.2
	Horizontal resolution	1 (longitude) × 0.5° (latitude, smoothly decreasing to 0.3° toward the equator) grids
	Vertical levels	52 levels with a bottom boundary layer
Sea ice model	Model type	Dynamical sea ice model
Coupling	Coupling interval	1 hour
	Flux adjustment	None
Forecast period	7 months	
Model run frequency	Once every 5 days	
Perturbation generator	Combination of the breeding of growing mode (BGM) method and the LAF method	
Initial atmospheric conditions	Near-real-time operation of JRA-55 (Kobayashi et al. 2015)	
Initial ocean conditions	MOVE/MRI.COM-G2 (Toyoda et al. 2013)	
Ensemble size	51 members per month	

Hindcast	Two initial dates per month for the 36 years from 1979 to 2014 Ensemble size: five for each initial date Ensemble generated via combined application of BGM and LAF methods
Timing of anomaly prediction for the next month/season	Variable (around the 20th of the month)
Forecast anomaly determination method	Against climatology (30-year average for the period from 1981 to 2010)
URL	http://ds.data.jma.go.jp/tcc/tcc/index.html
Contact	tcc@met.kishou.go.jp

4.7.2 Operationally available EPS LRF products

JMA provides gridded data and map products for three-month forecasts every month. Warm-season (June-July-August; JJA) forecasts are issued in February, March and April, and cold-season (December-January-February; DJF) forecasts are issued in September and October.
A model systematic bias was estimated for use as an average forecast error calculated from hindcast experiments for the 30 years from 1981 to 2010. The bias is removed from forecast fields, and grid-point values are processed to produce several forecast materials such as ensemble means and spreads.

The following model output products (Tables 4.7.2-1 and 4.7.2-2) for three-month and warm/cold-season forecasts are provided via the Tokyo Climate Center (TCC) website (http://ds.data.jma.go.jp/tcc/tcc/index.html).

Table 4.7.2-1 Gridded data products (GRIB2) for three-month and warm/cold-season forecasts provided via the TCC website

Details		Level (hPa)	Area	Base time & forecast time
Ensemble mean, its anomaly, and spread (standard deviation) values of forecast members	Sea level pressure*, its anomaly and spread	-	Global 2.5° × 2.5°	Base time: 00 UTC around the 15th of each month Forecast times: One- and three-month averages for targeted terms
	Rainfall amount, its anomaly and spread	-		
	Sea surface temperature* and its anomaly	-		
	Temperature*, its anomaly and spread	Surf, 850		
	Geopotential height*, its anomaly and spread	500		
	Wind (u, v), its anomaly and spread	850, 200		
Individual ensemble members	Sea level pressure* and its anomaly	-		Base time: 00 UTC on each initial date of prediction (every 5 days)
	Rainfall amount and its anomaly	-		
	Sea surface temperature* and its anomaly	-		

	Temperature* and its anomaly	Surf, 850, 500, 200		Forecast times: One-month averages for targeted terms
	Relative humidity and its anomaly	850		
	Specific humidity and its anomaly	850		
	Geopotential height* and its anomaly	850, 500, 300, 200, 100		
	Wind (u,v) and its anomaly	850, 500, 200		

* Geopotential height, sea level pressure, temperature and sea surface temperature are calibrated by subtracting the systematic error from the direct model output.

Table 4.7.2-2 Map products for three-month and warm/cold-season forecasts provided via the TCC website
<http://ds.data.jma.go.jp/tcc/tcc/products/model/map/4mE/index.html>

	Forecast time	Parameter
Ensemble mean, its anomaly and spread	Three-month forecast: Averages of first month, second month, third month, and three months Warm/cold season forecast: Averages of three months (JJA or DJF)	Geopotential height at 500 hPa, related anomaly and spread Temperature at 850 hPa, its anomaly and spread Sea level pressure, its anomaly and spread Stream function at 200 hPa, its anomaly and spread Stream function at 850 hPa, its anomaly and spread Wind (u,v) anomaly at 850 hPa Velocity potential at 200 hPa, its anomaly and spread Precipitation, its anomaly and spread Temperature at 2 m, its anomaly and spread Sea surface temperature and its anomaly

Table 4.7.2-3 SST Index Time Series
<http://ds.data.jma.go.jp/tcc/tcc/products/model/indices/3-mon/indices1/shisu_forecast.php>

Index	Description	Coordinates
Niño.1+2	Region off coasts of Peru and Chile	90°W – 80°W, 10°S – 0°
Niño.3	Eastern/Central Tropical Pacific	150°W – 90°W, 5°S – 5°N
Niño3.4	Central Tropical Pacific	170°W – 120°W, 5°S – 5°N
Niño.4	Western/Central Tropical Pacific	160°E – 150°W, 5°S – 5°N
TNA	Tropical North Atlantic	55°W – 15°W, 5°N – 25°N
TSA	Tropical South Atlantic	30°W – 10°E, 20°S – 0°
TAD	Tropical Atlantic Dipole	TNA – TSA
WTIO	Western Tropical Indian Ocean	50°E – 70°E, 10°S – 10°N
SETIO	Southeastern Tropical Indian Ocean	90°E – 110°E, 10°S – 0°
IOD	Indian Ocean Dipole	WTIO – SETIO

5. Verification of prognostic products

5.1 Annual verification summary

5.1.1 NWP prognostic products

Prognostic products are objectively verified against analysis and radiosonde observations according to the WMO/CBS standardized procedures for verification of deterministic NWP products as defined

in the Manual on the Global Data-processing and Forecasting System.

The results of monthly verification for 2019 are presented in Tables 5.1.1-1 – 5.1.1-20. All verification scores are only for prediction from 1200 UTC initials, and are computed using procedures approved at the 16th WMO Congress in 2011.

Table 5.1.1-1 Root mean square errors of geopotential height at 500 hPa against analysis (m)

Northern Hemisphere (20–90˚N)

Hours	Jan	Feb	Mar	Apr	May	Jun	Jul	Aug	Sep	Oct	Nov	Dec	Annual
24	7.9	7.9	7.1	6.7	6.2	6.2	5.7	5.7	6.1	6.3	6.8	7.3	6.7
72	26.2	28.2	25.8	23.7	20.9	19.8	17.3	17.8	19.6	21.2	21.9	23.4	22.3
120	52.5	52.4	52.8	47.1	42.4	37.3	34.7	35.1	41.9	42.9	46.9	47.4	44.8

Table 5.1.1-2 Root mean square errors of geopotential height at 500 hPa against analysis (m)

Southern Hemisphere (20–90˚S)

Hours	Jan	Feb	Mar	Apr	May	Jun	Jul	Aug	Sep	Oct	Nov	Dec	Annual
24	7.3	7.6	7.6	8.0	8.3	8.8	8.9	9.2	8.7	8.2	7.6	6.9	8.1
72	22.9	24.1	26.0	28.0	29.2	32.2	31.9	32.8	29.8	27.5	24.6	23.6	27.9
120	45.0	48.6	51.2	54.2	58.7	64.6	62.2	64.6	59.5	53.5	47.4	46.1	55.1

Table 5.1.1-3 Root mean square errors of geopotential height at 500 hPa against observations (m)

North America

Hours	Jan	Feb	Mar	Apr	May	Jun	Jul	Aug	Sep	Oct	Nov	Dec	Annual
24	12.5	12.1	11.3	11.5	10.1	10.0	9.5	10.2	10.2	11.3	12.2	11.8	11.1
72	31.4	29.9	25.4	24.7	20.7	18.9	15.8	16.2	20.1	25.1	24.1	25.7	23.6
120	55.8	57.1	49.7	46.7	38.1	35.7	26.6	31.5	37.0	44.6	56.8	48.5	45.0
ob. num.	86	85	86	86	86	86	87	85	85	85	86	86	

Table 5.1.1-4 Root mean square errors of geopotential height at 500 hPa against observations (m)

Europe/North Africa

Hours	Jan	Feb	Mar	Apr	May	Jun	Jul	Aug	Sep	Oct	Nov	Dec	Annual
24	16.0	13.9	13.0	10.6	9.5	8.8	8.2	8.1	11.0	11.6	13.0	14.7	11.8
72	32.6	30.6	31.9	25.6	21.8	19.4	20.9	16.8	22.9	25.2	30.0	29.2	26.0
120	67.7	56.3	59.8	49.7	46.0	33.1	34.3	33.4	52.4	55.1	50.6	57.4	50.8
ob. num.	52	53	51	49	52	52	52	52	51	52	53	51	

Table 5.1.1-5 Root mean square errors of geopotential height at 500 hPa against observations (m)

Asia

Hours	Jan	Feb	Mar	Apr	May	Jun	Jul	Aug	Sep	Oct	Nov	Dec	Annual
24	13.8	14.2	12.8	12.9	12.2	11.6	11.6	11.5	11.1	11.5	12.7	12.7	12.4
72	23.6	23.0	22.5	23.8	21.8	20.7	18.8	18.1	19.5	18.9	22.1	21.7	21.3
120	39.9	41.5	38.7	40.2	39.0	31.6	29.8	28.0	33.6	36.8	38.0	37.5	36.4
ob. num.	121	120	121	117	116	115	113	115	115	114	112	113	

Table 5.1.1-6 Root mean square errors of geopotential height at 500 hPa against observations (m)

Australia/New Zealand

Hours	Jan	Feb	Mar	Apr	May	Jun	Jul	Aug	Sep	Oct	Nov	Dec	Annual
24	17.4	16.9	16.5	14.5	14.5	14.1	13.3	14.2	13.7	13.8	14.5	14.8	14.9
72	22.7	22.1	23.7	25.2	22.1	25.4	24.0	28.9	26.0	20.7	22.5	23.2	24.0
120	36.6	38.8	35.4	41.3	46.5	53.9	48.3	55.5	47.8	39.8	37.5	39.2	43.9
ob. num.	14	14	14	13	13	12	12	12	12	12	12	13	

Table 5.1.1-7 Root mean square errors of geopotential height at 500 hPa against observations (m)

Northern Hemisphere (20–90˚N)

Hours	Jan	Feb	Mar	Apr	May	Jun	Jul	Aug	Sep	Oct	Nov	Dec	Annual
24	13.6	13.6	12.8	12.2	11.5	11.3	10.7	11.1	11.2	11.7	12.4	13.0	12.1
72	28.3	28.1	27.0	25.0	22.3	21.0	19.5	19.4	21.1	23.3	24.7	25.5	23.9
120	52.7	52.6	50.6	45.3	41.6	35.6	34.3	33.7	41.6	45.6	47.6	47.2	44.5
ob. num.	368	362	364	360	361	360	358	359	356	358	357	352	

Table 5.1.1-8 Root mean square errors of geopotential height at 500 hPa against observations (m)

Southern Hemisphere (20–90˚S)

Hours	Jan	Feb	Mar	Apr	May	Jun	Jul	Aug	Sep	Oct	Nov	Dec	Annual
24	13.4	12.6	13.1	13.3	12.5	13.2	13.3	13.6	12.2	13.1	13.2	12.7	13.0
72	20.3	21.5	22.7	24.4	26.0	27.4	28.1	29.5	24.6	24.0	22.0	21.1	24.5
120	35.4	38.9	38.2	41.7	47.4	49.5	49.0	50.9	47.6	41.2	37.9	35.1	43.1
ob. num.	44	43	42	39	40	39	39	39	40	40	40	44	

Table 5.1.1-9 Root mean square of vector wind errors at 250 hPa against analysis (m/s)

Northern Hemisphere (20–90˚N)

Hours	Jan	Feb	Mar	Apr	May	Jun	Jul	Aug	Sep	Oct	Nov	Dec	Annual
24	3.5	3.7	3.5	3.6	3.6	3.6	3.6	3.5	3.5	3.4	3.4	3.3	3.5
72	7.7	8.6	8.3	8.2	8.1	8.3	8.2	8.1	8.2	8.0	7.8	7.6	8.1
120	13.0	13.6	14.1	13.5	13.2	12.9	12.6	12.8	13.8	13.3	13.3	12.7	13.2

Table 5.1.1-10 Root mean square of vector wind errors at 250 hPa against analysis (m/s)

Southern Hemisphere (20–90˚S)

Hours	Jan	Feb	Mar	Apr	May	Jun	Jul	Aug	Sep	Oct	Nov	Dec	Annual
24	3.3	3.4	3.5	3.6	3.5	3.7	3.5	3.4	3.4	3.4	3.4	3.4	3.5
72	8.3	8.5	8.6	9.0	8.7	9.3	8.9	8.8	8.3	8.2	8.1	8.0	8.6
120	13.7	14.0	14.2	14.5	14.9	15.7	14.5	14.3	13.9	13.2	13.1	13.1	14.1

Table 5.1.1-11 Root mean square of vector wind errors at 250 hPa against observations (m/s)

North America

Hours	Jan	Feb	Mar	Apr	May	Jun	Jul	Aug	Sep	Oct	Nov	Dec	Annual
24	6.3	6.1	5.7	6.1	6.2	6.4	5.3	5.7	5.6	5.6	5.7	5.4	5.8
72	11.3	11.0	9.7	10.1	10.3	9.9	8.9	9.3	9.6	10.0	9.8	9.7	10.0
120	17.7	17.0	15.9	16.0	14.9	14.1	12.4	14.0	14.3	15.7	16.9	16.1	15.5
ob. num.	84	84	84	85	85	86	87	86	87	86	87	88	

Table 5.1.1-12 Root mean square of vector wind errors at 250 hPa against observations (m/s)

Europe/North Africa

Hours	Jan	Feb	Mar	Apr	May	Jun	Jul	Aug	Sep	Oct	Nov	Dec	Annual
24	4.7	4.9	4.7	4.6	5.0	4.7	4.8	4.8	5.1	5.2	5.3	5.5	4.9
72	8.7	10.2	10.1	8.7	8.9	7.5	9.0	8.1	10.3	10.1	10.3	10.3	9.4
120	16.9	16.1	17.3	14.7	14.6	12.0	14.1	13.5	18.0	16.4	15.8	17.1	15.6
ob. num.	55	56	54	52	55	55	55	55	55	55	56	54	

Table 5.1.1-13 Root mean square of vector wind errors at 250 hPa against observations (m/s)

Asia

Hours	Jan	Feb	Mar	Apr	May	Jun	Jul	Aug	Sep	Oct	Nov	Dec	Annual
24	4.8	6.0	5.8	6.7	6.2	6.8	6.4	5.5	5.4	5.2	5.0	4.5	5.7
72	7.2	8.6	8.9	10.1	10.2	11.5	10.3	9.2	8.8	8.3	7.7	7.1	9.1
120	10.3	12.3	12.4	13.8	14.0	14.2	13.7	12.6	12.9	12.9	11.0	10.2	12.6
ob. num.	141	138	139	135	136	133	134	135	135	136	133	133	

Table 5.1.1-14 Root mean square of vector wind errors at 250 hPa against observations (m/s)

Australia/New Zealand

Hours	Jan	Feb	Mar	Apr	May	Jun	Jul	Aug	Sep	Oct	Nov	Dec	Annual
24	5.6	5.1	6.2	5.3	4.9	5.4	5.3	5.1	5.2	5.6	5.8	6.2	5.5
72	8.2	7.8	9.9	9.1	8.4	9.1	8.6	8.1	7.7	7.7	9.5	8.9	8.6
120	12.6	13.2	13.9	12.7	13.2	17.1	13.7	11.6	12.0	12.0	12.3	13.3	13.2
ob. num.	15	15	15	14	14	13	13	13	13	13	13	14	

Table 5.1.1-15 Root mean square of vector wind errors at 250 hPa against observations (m/s)

Northern Hemisphere (20–90˚N)

Hours	Jan	Feb	Mar	Apr	May	Jun	Jul	Aug	Sep	Oct	Nov	Dec	Annual
24	5.0	5.5	5.3	5.8	5.6	5.9	5.5	5.2	5.1	5.0	4.9	4.8	5.3
72	8.5	9.5	9.1	9.4	9.4	9.7	9.4	9.0	9.1	8.9	8.6	8.4	9.1
120	13.7	14.5	14.5	14.2	13.9	13.5	13.4	13.4	14.5	14.3	13.6	13.5	13.9
ob. num.	386	382	384	378	381	379	382	383	383	384	382	380	

Table 5.1.1-16 Root mean square of vector wind errors at 250 hPa against observations (m/s)

Southern Hemisphere (20–90˚S)

Hours	Jan	Feb	Mar	Apr	May	Jun	Jul	Aug	Sep	Oct	Nov	Dec	Annual
24	4.9	5.3	5.7	5.8	5.7	5.5	5.7	5.7	5.5	5.7	5.6	5.6	5.6
72	8.1	9.1	9.0	10.6	9.3	9.2	9.9	9.4	8.9	9.0	8.7	8.5	9.2
120	12.1	13.7	13.4	15.3	14.2	15.6	14.4	13.9	13.8	12.9	11.9	13.4	13.8
ob. num.	48	46	45	39	41	41	42	42	42	42	42	45	

Table 5.1.1-17 Root mean square of vector wind errors at 850 hPa against analysis (m/s)

Tropic

Hours	Jan	Feb	Mar	Apr	May	Jun	Jul	Aug	Sep	Oct	Nov	Dec	Annual
24	1.6	1.6	1.5	1.4	1.4	1.5	1.5	1.6	1.6	1.5	1.5	1.5	1.5
72	2.8	2.8	2.6	2.4	2.5	2.7	2.8	2.8	2.9	2.7	2.7	2.7	2.7
120	3.6	3.6	3.4	3.0	3.0	3.3	3.5	3.5	3.8	3.4	3.4	3.4	3.4

Table 5.1.1-18 Root mean square of vector wind errors at 250 hPa against analysis (m/s)

Tropic

Hours	Jan	Feb	Mar	Apr	May	Jun	Jul	Aug	Sep	Oct	Nov	Dec	Annual
24	3.4	3.3	3.1	3.0	3.0	3.3	3.3	3.4	3.3	2.9	3.1	3.1	3.2
72	6.2	5.9	5.7	5.4	5.2	6.1	5.7	5.8	5.6	5.1	5.5	5.4	5.6
120	8.1	7.7	7.4	7.1	6.8	7.7	7.2	7.4	7.2	6.7	7.0	7.0	7.3

Table 5.1.1-19 Root mean square of vector wind errors at 850 hPa against observations (m/s)

Tropic

Hours	Jan	Feb	Mar	Apr	May	Jun	Jul	Aug	Sep	Oct	Nov	Dec	Annual
24	3.6	3.3	3.4	3.1	3.2	3.3	3.3	3.5	3.4	3.1	3.2	3.3	3.3
72	4.3	3.8	4.0	3.6	3.7	3.9	3.9	4.1	4.0	3.6	4.0	3.9	3.9
120	4.8	4.3	4.5	4.0	4.0	4.4	4.6	4.8	4.5	4.1	4.6	4.3	4.4
ob. num.	64	65	65	66	71	70	72	71	70	69	69	71	

Table 5.1.1-20 Root mean square of vector wind errors at 250 hPa against observations (m/s)

Tropic

Hours	Jan	Feb	Mar	Apr	May	Jun	Jul	Aug	Sep	Oct	Nov	Dec	Annual
24	5.1	4.7	4.8	4.5	4.5	4.6	4.8	5.3	5.0	4.2	4.6	4.5	4.7
72	6.9	6.2	6.2	5.9	6.0	6.5	6.7	7.4	7.0	5.7	6.2	5.8	6.4
120	8.1	7.3	7.3	7.0	7.3	7.9	8.2	8.8	8.3	7.0	7.2	6.8	7.6
ob. num.	65	65	65	66	71	72	74	74	72	72	71	71	

The Global EPS is verified against analysis values in line with the Manual on GDPFS (WMO-No. 485). The Brier Skill Score (BSS) for seasonal (DJF: December-January-February; MAM: March-April-May; JJA: June-July-August; SON: September-October-November) and annual averages in 2019(December in 2018) are shown in Tables 5.1.1-21 – 5.1.1-26.

Table 5.1.1-21 BSS for geopotential height at 500 hPa over the Northern Hemisphere (20–90°N)

Hour	Z500 anomaly +1.0 standard deviation					Z500 anomaly +1.5 standard deviation					Z500 anomaly +2.0 standard deviation				
	DJF	MAM	JJA	SON	Annual	DJF	MAM	JJA	SON	Annual	DJF	MAM	JJA	SON	Annual
24	0.917	0.910	0.879	0.906	0.903	0.899	0.880	0.858	0.887	0.881	0.837	0.841	0.834	0.834	0.836
72	0.781	0.772	0.710	0.764	0.757	0.733	0.722	0.684	0.730	0.717	0.581	0.631	0.654	0.650	0.629
120	0.606	0.578	0.523	0.576	0.571	0.560	0.505	0.482	0.518	0.516	0.394	0.369	0.422	0.424	0.402
168	0.423	0.390	0.329	0.382	0.381	0.361	0.305	0.274	0.318	0.314	0.194	0.148	0.201	0.202	0.186
Hour	Z500 anomaly -1.0 standard deviation					Z500 anomaly -1.5 standard deviation					Z500 anomaly -2.0 standard deviation				
	DJF	MAM	JJA	SON	Annual	DJF	MAM	JJA	SON	Annual	DJF	MAM	JJA	SON	Annual
24	0.907	0.902	0.877	0.900	0.897	0.885	0.882	0.858	0.879	0.876	0.859	0.858	0.832	0.856	0.851
72	0.738	0.716	0.674	0.731	0.715	0.685	0.659	0.626	0.682	0.663	0.623	0.613	0.554	0.627	0.604
120	0.538	0.488	0.466	0.506	0.499	0.470	0.413	0.401	0.437	0.430	0.392	0.346	0.299	0.357	0.349
168	0.346	0.303	0.273	0.306	0.307	0.260	0.221	0.205	0.230	0.229	0.159	0.155	0.130	0.167	0.153

Table 5.1.1-22 BSS for temperature at 850 hPa over the Northern Hemisphere (20–90˚N)

Hour	T850 anomaly +1.0 standard deviation					T850 anomaly +1.5 standard deviation					T850 anomaly +2.0 standard deviation				
	DJF	MAM	JJA	SON	Annual	DJF	MAM	JJA	SON	Annual	DJF	MAM	JJA	SON	Annual
24	0.820	0.804	0.761	0.799	0.796	0.775	0.769	0.738	0.757	0.760	0.719	0.723	0.703	0.730	0.719
72	0.640	0.611	0.555	0.610	0.604	0.565	0.548	0.518	0.544	0.544	0.455	0.452	0.462	0.495	0.466
120	0.475	0.422	0.395	0.438	0.432	0.390	0.348	0.351	0.360	0.362	0.280	0.246	0.286	0.288	0.275
168	0.305	0.264	0.235	0.278	0.271	0.222	0.195	0.195	0.214	0.207	0.136	0.116	0.134	0.155	0.135
Hour	T850 anomaly -1.0 standard deviation					T850 anomaly -1.5 standard deviation					T850 anomaly -2.0 standard deviation				
	DJF	MAM	JJA	SON	Annual	DJF	MAM	JJA	SON	Annual	DJF	MAM	JJA	SON	Annual
24	0.825	0.825	0.765	0.820	0.809	0.787	0.777	0.717	0.771	0.763	0.745	0.731	0.670	0.709	0.714
72	0.652	0.635	0.545	0.652	0.621	0.606	0.569	0.471	0.583	0.557	0.563	0.519	0.393	0.501	0.494
120	0.474	0.454	0.360	0.483	0.443	0.417	0.386	0.273	0.395	0.368	0.383	0.332	0.219	0.296	0.307
168	0.289	0.291	0.200	0.305	0.271	0.241	0.231	0.130	0.210	0.203	0.179	0.170	0.090	0.108	0.137

Table 5.1.1-23 BSS for geopotential height at 500 hPa over the Tropics (20˚S–20˚N)

Hour	Z500 anomaly +1.0 standard deviation					Z500 anomaly +1.5 standard deviation					Z500 anomaly +2.0 standard deviation				
	DJF	MAM	JJA	SON	Annual	DJF	MAM	JJA	SON	Annual	DJF	MAM	JJA	SON	Annual
24	0.797	0.747	0.742	0.676	0.740	0.785	0.713	0.709	0.532	0.685	0.718	0.615	0.637	0.292	0.566
72	0.635	0.602	0.536	0.506	0.570	0.619	0.572	0.514	0.376	0.520	0.559	0.474	0.450	0.068	0.388
120	0.510	0.467	0.404	0.430	0.453	0.499	0.444	0.396	0.330	0.417	0.409	0.358	0.350	0.160	0.319
168	0.341	0.242	0.220	0.273	0.269	0.329	0.218	0.226	0.221	0.249	0.260	0.140	0.197	0.121	0.180
Hour	Z500 anomaly -1.0 standard deviation					Z500 anomaly -1.5 standard deviation					Z500 anomaly -2.0 standard deviation				
	DJF	MAM	JJA	SON	Annual	DJF	MAM	JJA	SON	Annual	DJF	MAM	JJA	SON	Annual
24	0.792	0.764	0.703	0.729	0.747	0.772	0.740	0.701	0.702	0.729	0.710	0.703	0.662	0.703	0.695
72	0.585	0.538	0.420	0.497	0.510	0.545	0.495	0.411	0.468	0.480	0.432	0.402	0.373	0.443	0.413
120	0.428	0.322	0.287	0.332	0.342	0.369	0.266	0.259	0.288	0.296	0.268	0.188	0.235	0.276	0.242
168	0.237	0.100	0.095	0.130	0.141	0.199	0.070	0.102	0.106	0.119	0.123	0.018	0.082	0.107	0.083

Table 5.1.1-24 BSS for temperature at 850 hPa over the Tropics (20˚S–20˚N)

Hour	T850 anomaly +1.0 standard deviation					T850 anomaly +1.5 standard deviation					T850 anomaly +2.0 standard deviation				
	DJF	MAM	JJA	SON	Annual	DJF	MAM	JJA	SON	Annual	DJF	MAM	JJA	SON	Annual
24	0.505	0.487	0.511	0.517	0.505	0.426	0.405	0.476	0.452	0.440	0.366	0.323	0.427	0.374	0.372
72	0.211	0.158	0.232	0.275	0.219	0.170	0.114	0.225	0.212	0.180	0.161	0.061	0.194	0.160	0.144
120	0.094	0.037	0.118	0.187	0.109	0.088	0.025	0.131	0.132	0.094	0.103	0.006	0.118	0.088	0.079

168	0.009	-0.043	0.048	0.119	0.033	0.026	-0.026	0.071	0.072	0.036	0.045	-0.023	0.059	0.030	0.028
Hour	T850 anomaly -1.0 standard deviation					T850 anomaly -1.5 standard deviation					T850 anomaly -2.0 standard deviation				
	DJF	MAM	JJA	SON	Annual	DJF	MAM	JJA	SON	Annual	DJF	MAM	JJA	SON	Annual
24	0.619	0.609	0.553	0.567	0.587	0.588	0.577	0.494	0.534	0.548	0.551	0.540	0.411	0.504	0.501
72	0.372	0.364	0.305	0.327	0.342	0.352	0.334	0.247	0.304	0.309	0.314	0.297	0.166	0.289	0.266
120	0.236	0.235	0.178	0.203	0.213	0.214	0.219	0.124	0.194	0.188	0.176	0.189	0.053	0.176	0.148
168	0.136	0.135	0.071	0.098	0.110	0.112	0.134	0.030	0.111	0.097	0.081	0.111	-0.017	0.105	0.070

Table 5.1.1-25 BSS for geopotential height at 500 hPa over the Southern Hemisphere (20–90˚S)

Hour	Z500 anomaly +1.0 standard deviation					Z500 anomaly +1.5 standard deviation					Z500 anomaly +2.0 standard deviation				
	DJF	MAM	JJA	SON	Annual	DJF	MAM	JJA	SON	Annual	DJF	MAM	JJA	SON	Annual
24	0.903	0.913	0.928	0.916	0.915	0.881	0.886	0.914	0.902	0.896	0.830	0.834	0.885	0.879	0.857
72	0.750	0.759	0.777	0.779	0.766	0.713	0.705	0.741	0.747	0.726	0.647	0.618	0.675	0.693	0.658
120	0.567	0.571	0.592	0.610	0.585	0.502	0.498	0.524	0.558	0.521	0.405	0.375	0.427	0.461	0.417
168	0.362	0.365	0.404	0.430	0.390	0.292	0.272	0.342	0.371	0.319	0.163	0.138	0.258	0.274	0.208
Hour	Z500 anomaly -1.0 standard deviation					Z500 anomaly -1.5 standard deviation					Z500 anomaly -2.0 standard deviation				
	DJF	MAM	JJA	SON	Annual	DJF	MAM	JJA	SON	Annual	DJF	MAM	JJA	SON	Annual
24	0.889	0.904	0.912	0.918	0.906	0.863	0.888	0.894	0.905	0.888	0.845	0.856	0.867	0.883	0.863
72	0.705	0.716	0.721	0.753	0.724	0.644	0.663	0.676	0.716	0.674	0.586	0.581	0.627	0.652	0.612
120	0.494	0.485	0.494	0.552	0.506	0.414	0.413	0.429	0.493	0.437	0.332	0.322	0.360	0.414	0.357
168	0.297	0.290	0.298	0.352	0.309	0.212	0.216	0.238	0.294	0.240	0.138	0.150	0.173	0.229	0.172

Table 5.1.1-26 BSS for temperature at 850 hPa over the Southern Hemisphere (20–90˚S)

Hour	T850 anomaly +1.0 standard deviation					T850 anomaly +1.5 standard deviation					T850 anomaly +2.0 standard deviation				
	DJF	MAM	JJA	SON	Annual	DJF	MAM	JJA	SON	Annual	DJF	MAM	JJA	SON	Annual
24	0.805	0.809	0.827	0.834	0.819	0.765	0.766	0.790	0.810	0.783	0.735	0.736	0.734	0.776	0.745
72	0.603	0.607	0.620	0.652	0.620	0.534	0.535	0.563	0.611	0.561	0.486	0.496	0.480	0.553	0.504
120	0.432	0.422	0.434	0.483	0.443	0.352	0.347	0.371	0.433	0.376	0.294	0.288	0.280	0.364	0.306
168	0.275	0.258	0.274	0.316	0.281	0.206	0.197	0.224	0.273	0.225	0.141	0.146	0.153	0.213	0.163
Hour	T850 anomaly -1.0 standard deviation					T850 anomaly -1.5 standard deviation					T850 anomaly -2.0 standard deviation				
	DJF	MAM	JJA	SON	Annual	DJF	MAM	JJA	SON	Annual	DJF	MAM	JJA	SON	Annual
24	0.800	0.822	0.835	0.845	0.825	0.768	0.781	0.796	0.802	0.787	0.739	0.724	0.715	0.727	0.726
72	0.604	0.625	0.644	0.662	0.634	0.567	0.567	0.602	0.601	0.584	0.535	0.495	0.522	0.521	0.519
120	0.426	0.428	0.439	0.471	0.441	0.395	0.363	0.386	0.405	0.387	0.373	0.300	0.298	0.317	0.322
168	0.270	0.255	0.269	0.298	0.273	0.239	0.199	0.212	0.240	0.223	0.210	0.127	0.133	0.173	0.161

5.2 Research performed in this field

6. Plans for the future (next 4 years)

6.1 Development of the GDPFS

6.1.1 Major changes expected in the next year

(1) GOES-16 AMV data will be incorporated into the global NWP system.
(2) CSR data collected from Himawari-8 bands 9 and 10 will be incorporated into the local NWP system.
(3) Metop-C/AMSU-A and MHS data will be incorporated into the global NWP system.
(4) ScatSat-1/OSCAT wind data will be incorporated into the global NWP system.
(5) Two-tiered SST approach (using precomputed SST from the Seasonal EPS) will be implemented into the Global EPS in the tropics and subtropics for forecasts longer than 12 days.
(6) The forecast model adopted in the GEPS will be replaced with the latest operational GSM.
(7) LETKF-based initial perturbations of the Global EPS will be produced from the hybrid data assimilation cycle of the global NWP system. SV-based initial perturbations of the system will also be improved.
(8) High-resolution and highly accurate sea surface temperature data based on Himawari-8 observation will be incorporated into lower-boundary conditions for the MSM and the LFM.
(9) The physics parameterization of the global NWP system and GEPS will be upgraded.
(10) The GSM forecast range will be extended from 132 to 264 hours at 00 UTC initial times.
(11) A new coastal ocean analysis/forecasting system (MOVE/MRI.COM-JPN) with a high-resolution (2 km) forecast model covering the whole of the Japanese coast and a 4D-Var assimilation system covering the North Pacific will be put into operation.
(12) The grid resolution of the Wave Ensemble System (WENS) will be enhanced from 140 to 55 km, and shallow-water effects will be incorporated.
(13) The 2D-Var data assimilation system will be adopted in aerosol (Aeolian dust) analysis.
(14) The horizontal resolution of the regional chemical transport model will be enhanced from 20 to 5 km.

6.1.2 Major changes expected in the next four years

(1) The vertical layers of the global NWP system and GEPS will be enhanced.
(2) The horizontal resolutions of the GSM and GEPS will be improved.
(3) The forecast model adopted in the GEPS will be replaced with the latest operational GSM.
(4) The number of GEPS and WENS members will be increased.
(5) The number of ensemble members used to create flow-dependent background error covariances in GA will be increased.
(6) A soil moisture analysis system will be incorporated into GA.

(7) Improvements to observation processing (such as snow cover estimation from satellite observations) will be incorporated into snow depth analysis.
(8) The physical processes of the MSM and LFM will be upgraded.
(9) The number of vertical layers in the LFM will be enhanced from 58 to 76.
(10) The number of vertical layers in the MSM will be enhanced from 76 to 96.
(11) A new framework for a data assimilation system (ASUCA-Var) will be incorporated into the mesoscale NWP system.
(12) The horizontal and vertical resolutions of Hourly Analysis will be enhanced, and the number of related daily operations will be increased.
(13) GOES-17 AMV and CSR data will be incorporated into the global NWP system.
(14) Metop-C/GRAS data will be incorporated into the global NWP system.
(15) Metop-C/IASI data will be incorporated into the global NWP system.
(16) Accounting for inter-channel error correlations in the assimilation of satellite radiances will be incorporated into the global NWP system.
(17) GNSS-RO bending-angle data from TanDEM-X/IGOR will be assimilated into the global NWP system
(18) The satellite radiance data used in the global NWP system (e.g., ATMS, CrIS, IASI, AIRS) will be assimilated into the mesoscale and local NWP systems.
(19) More satellite data, including ScatSat-1/OSCAT and VIIRS-AMV content, will be assimilated into the global, mesoscale and local NWP systems.
(20) Modification to enhance the use of aircraft data will be incorporated into the global NWP system.
(21) GPS radiosonde data on drift positions will be assimilated into the global NWP system.
(22) Modification to enhance the use of land surface observations on a temporal scale will be incorporated into the global NWP system.
(23) Metop-C/ASCAT wind data will be incorporated into the mesoscale NWP system.
(24) The 2D-Var data assimilation system will be adopted in stratospheric ozone analysis.
(25) The regional chemical transport model run frequency will be increased from once to three times a day.
(26) The vertical resolution of the chemical transport model in the UV prediction system will be enhanced from 64 to 100 levels.
(27) The grid resolution of the Global Wave Model (GWM) will be enhanced from 55 to 25 km.
(28) A new wave model with a 1-minute grid resolution for coastal sea areas of Japan will be put into operation.
(29) The forecast period for both storm surge models will be extended from 39 to 51 hours for the Japan region and from 72 to 132 hours for the Asian region.
(30) A new storm surge model involving the use of an unstructured grid will be incorporated, and grid resolution will be enhanced in both storm surge models.
(31) Storm surge EPSs will be incorporated into both storm surge models.
(32) An incremental 4DVAR method will be adopted for the global ocean data assimilation system (MOVE/MRI.COM) with resolution increased to 0.25 × 0.25°.

(33) The representation of physical processes and the model resolution for the Seasonal EPS will be improved.

(34) The results of the third Japanese global atmospheric reanalysis (the Japanese Reanalysis for Three Quarters of a Century; JRA-3Q, being produced with the TL479 version of JMA's operational data assimilation system as of December 2018) will be made available.

6.2 Planned research Activities in NWP, Nowcasting, Long-range Forecasting and Specialized Numerical Predictions

6.2.1 Planned Research Activities in NWP

6.2.2 Planned Research Activities in Nowcasting

(1) Use of dual polarized radar data for R/A, VSRF, Thunder Nowcasts and Hazardous Wind Potential Nowcasts

6.2.3 Planned Research Activities in Long-range Forecasting

6.2.4 Planned Research Activities in Specialized Numerical Predictions

(1) Time-of-arrival products for nuclear environmental emergency response

In line with a development plan set by the CBS expert team on Emergency Response Activities (ET-ERA), JMA is currently researching time-of-arrival products. These exhibited the highest demand in a 2016 Regional Association II (Asia) user request survey.

(2) Probability forecasts for volcanic ash

JMA is currently exploring methods to meet the needs of probability forecasts for volcanic ash as described in the International Airways Volcano Watch (IAVW) roadmap.

7. References

Aoki, Te., Ta. Aoki, M. Fukabori and T. Takao, 2002: Characteristics of UV-B Irradiance at Syowa Station, Antarctica: Analyses of the Measurements and Comparison with Numerical Simulations. *J. Meteor. Soc. Japan.*, **80**, 161–170.

Aranami, K., T. Hara, Y. Ikuta, K. Kawano, K. Matsubayashi, H. Kusabiraki, T. Ito, T. Egawa, K. Yamashita, Y. Ota, Y. Ishikawa, T. Fujita, and J. Ishida, 2015: A new operational regional model for convection-permitting numerical weather prediction at JMA. *CAS/JSC WGNE Res. Activ. Atmos. Oceanic Modell.*, 45, 5.05-5.06.

Bauer, P., E. Moreau, F. Chevallier, and U. O'Keeffe, 2006: Multiple-scattering microwave radiative transfer for data assimilation applications. Quart. J. Roy. Meteorol. Soc. 132, 1259-1281

Buizza, R. and T. N. Palmer, 1995: The singular-vector structure of the atmospheric global circulation. *J. Atmos. Sci.*, **52**, 1434–1456.

Deushi, M., and K. Shibata, 2011: Development of an MRI Chemistry-Climate Model ver. 2 for the study of tropospheric and stratospheric chemistry, *Papers in Meteorology and Geophysics,* **62**, 1 – 46.

Egbert, G. and S. Erofeeva, 2002: Efficient Inverse Modeling of Barotropic Ocean Tides. *J. Atmos. Oceanic Technol.*, **19**, 183–204.

Ehrendorfer, M., R. M. Errico and K. D. Raeder, 1999: Singular-Vector Perturbation Growth in a Primitive Equation Model with Moist Physics. *J. Atmos. Sci.*, **56**, 1627–1648.

Foster, D. J. and R. D. Davy, 1988: *Global Snow Depth Climatology.* USAF-ETAC/TN-88/006. Scott Air Force Base, Illinois, p. 48.

Geer, A. J. and P. Bauer, 2011: Observation errors in all-sky data assimilation. Quart. J. Roy. Meteorol. Soc. 137, 2024-2037

Hasegawa, Y., A. Sugai, Yo. Hayashi, Yu. Hayashi, S. Saito and T. Shimbori, 2015: Improvements of volcanic ash fall forecasts issued by the Japan Meteorological Agency. *J. Appl. Volcanol.*, **4**: 2.

Hamrud, M., M. Bonavita, and L. Isaksen, 2015: EnKF and hybrid gain ensemble data assimilation. Part I: EnKF implementation. *Mon. Wea. Rev.*, **143**, 4847–4864.

Hirahara, Y., T. Egawa and M. Kazumori, 2017: Operational use of Suomi NPP ATMS radiance data in JMA's global NWP system. CAS/JSC WGNE Research Activities in Atmospheric and Oceanic Modelling, Rep., 47, 1 – 13.

Honda, Y., M. Nishijima, K. Koizumi, Y. Ohta, K. Tamiya, T. Kawabata and T. Tsuyuki, 2005: A pre-operational variational data assimilation system for a non-hydrostatic model at the Japan Meteorological Agency: Formulation and preliminary results. *Quart. J. Roy. Meteor. Soc.*, **131**, 3465-3475.

Hunt, B. R., E. J. Kostelich, and I. Szunyogh, 2007: Efficient data assimilation for spatiotemporal chaos: A local ensemble transform Kalman filter. *Physica D*, **230**, 112–126.

Ishida, J., C. Muroi, and Y. Aikawa, 2009: Development of a new dynamical core for the nonhydrostatic model. *CAS/JSC WGNE Res. Activ. Atmos. Oceanic Modell.*, **39**, 05.09–05.10.

Ishida, J., C. Muroi, K. Kawano, and Y. Kitamura, 2010: Development of a new nonhydrostatic model "ASUCA" at JMA. *CAS/JSC WGNE Res. Activ. Atmos. Oceanic Modell.*, **40**, 05.11–05.12.

Ishikawa, Y. and K. Koizumi, 2002: Meso-scale analysis. *In Outline of the Operational Numerical Weather Prediction at the Japan Meteorological Agency. Appendix to WMO Technical Progress Report on the Global Data-processing and Forecasting Systems (GDPFS) and Numerical Weather Prediction (NWP) Research*. Japan Meteorological Agency, Tokyo, Japan, 26–31. (http://warp.da.ndl.go.jp/info:ndljp/pid/246209/www.jma.go.jp/jma/jma-eng/jma-center/nwp/outline-nwp/index.htm)

JMA., 2019: Computer System, In Outline of the Operational Numerical Weather Prediction at the Japan Meteorological Agency. Appendix to WMO Technical Progress Report on the Global Data-

processing and Forecasting Systems (GDPFS) and Numerical Weather Prediction (NWP) Research. Japan Meteorological Agency, Tokyo, Japan, 1–7. (http://www.jma.go.jp/jma/jma-eng/jma-center/nwp/outline2019-nwp/index.htm)

Kajino, M., M. Deushi, T. T. Sekiyama, N. Oshima, K. Yumimoto, T. Y. Tanaka, J. Ching, A. Hashimoto, T. Yamamoto, M. Ikegami, A. Kamada, M. Miyashita, Y. Inomata, S. Shima, A. Takami, A. Shimizu, S. Hatakeyama, Y. Sadanaga, H. Irie, K. Adachi, Y. Zaizen, Y. Igarashi, H. Ueda, T. Maki, M. Mikami, 2019: NHM-Chem, the Japan Meteorological Agency's regional meteorology – chemistry model: model evaluations toward the consistent predictions of the chemical, physical, and optical properties of aerosols, J. Meteor. Soc. Japan, 97(2), 337-374.

Kamekawa, N. and M. Kazumori, 2017: Assimilation of Suomi NPP/CrIS radiance data into JMA's global NWP system. CAS/JSC WGNE Research Activities in Atmospheric and Oceanic Modelling, Rep., 47, 1 – 17.

Kazumori, M., T. Kadowaki, 2017: Development of an all-sky assimilation of microwave imager and sounder radiances for the Japan Meteorological Agency global numerical weather prediction system. Tech. Proc. of 21st International TOVS Study Conference, Darmstadt, Germany 29 November – 5 December 2017.

Kobayashi, S., Y. Ota, Y. Harada, A. Ebita, M. Moriya, H. Onoda, K. Onogi, H. Kamahori, C. Kobayashi, H. Endo, K. Miyaoka and K. Takahashi, 2015: The JRA-55 reanalysis: General specifications and basic characteristics. *J. Meteor. Soc. Japan*, **93**, 5-48.

Kohno, N., D. Miura, and K. Yoshita, 2012: The Development of JMA Wave Data Assimilation System. Proceeding of 12th International Workshop on Wave Hindcasting and Forecasting & 3rd Coastal Hazard Symposium, H2.
(http://www.waveworkshop.org/12thWaves/papers/full_paper_Kohno_et_al.pdf)

Koren, B., 1993: A Robust Upwind Discretization Method For Advection, Diffusion And Source Terms. *CWI Technical Report NM-R* **9308**, 1-22.

Kurihara Y, Murakami H and Kachi M., 2016: Sea surface temperature from the new Japanese geostationary meteorological Himawari-8 satellite, Geophysical Research Letters, 43(3), 1234-40.

Lorenc, A. C., 2003. The potential of the ensemble Kalman filter for NWP: a comparison with 4D-Var. Quart. J. Roy. Meteor. Soc., 129, 3183 – 3203.

Nakamura, T., H. Akiyoshi, M. Deushi, K. Miyazaki, C. Kobayashi, K. Shibata, and T. Iwasaki, 2013: A multimodel comparison of stratospheric ozone data assimilation based on an ensemble Kalman filter approach, *J. Geophys. Res. Atmos.*, **118**, 3848-3868, doi:10.1002/jgrd.50338.

Okabe, I., 2019: Operational use of surface-sensitive Clear-Sky Radiance (CSR) data in JMA's Global NWP System. CAS/JSC WGNE Research Activities in Atmospheric and Oceanic Modelling, Rep. 49, 1.15-1.16.

Onogi, K., J. Tsutsui, H. Koide, M. Sakamoto, S. Kobayashi, H. Hatsushika, T. Matsumoto, N. Yamazaki, H. Kamahori, K. Takahashi, S. Kadokura, K. Wada, K. Kato, R. Oyama, T. Ose, N. Mannoji, and R. Taira, 2007: The JRA-25 reanalysis. *J. Meteor. Soc. Japan*, **85**, 369-432.

Ono, K., Y. Honda, M. Kunii 2011: A mesoscale ensemble prediction system using singular vector

methods. *CAS/JSC WGNE Res. Activ. Atmos. Oceanic Modell.*, **41**, 5.17-5.18.

Ono, K., 2017: Consistent Initial and Lateral Boundary Perturbations in Mesoscale Ensemble Prediction System at JMA. CAS/JSC WGNE Res. Activ. Atmos. Oceanic Modell., **47**, 5.16-5.17.

Palmer, T. N., R. Buizza, F. Doblas-Reyes, T. Jung, M. Leutbecher, G. J. Shutts, M. Steinheimer, and A. Weisheimer, 2009: Stochastic parametrization and model uncertainty. *ECMWF Technical Memoranda*, **598**, 42pp.

Saito, K., T. Fujita, Y. Yamada, J. Ishida, Y. Kumagai, K. Aranami, S. Ohmori, R. Nagasawa, S. Kumagai, C. Muroi, T. Kato, H. Eito and Y. Yamazaki, 2006: The operational JMA Nonhydrostatic Mesoscale Model. *Mon. Wea. Rev.*, **134**, 1266-1298.

Saito, K., J. Ishida, K. Aranami, T. Hara, T. Segawa, M. Narita, and Y. Honda, 2007: Nonhydrostatic Atmospheric Models and Operational Development at JMA. *J. Meteor. Soc. Japan*, **85B**, 271-304.

Sako, H.: 2010: Assimilation of aircraft temperature data in the JMA global 4D-Var data assimilation system, CAS/JSC WGNE Research Activities in Atmospheric and Oceanic Modelling, 40, 1 – 33.

Sekiyama, T. T., Tanaka, T. Y., Shimizu, A., and Miyoshi, T., 2010: Data assimilation of CALIPSO aerosol observations, *Atmos. Chem. Phys.*, **10**, 39-49.

Sekiyama, T. T., K. Yumimoto, T. Y. Tanaka, T. Nagao, M. Kikuchi, and H. Murakami, 2016: Data Assimilation of Himawari-8 Aerosol Observations: Asian Dust Forecast in June 2015, *SOLA*, **12**, 86–90.

Shimbori, T., Y. Aikawa and N. Seino, 2009: Operational implementation of the tephra fall forecast with the JMA mesoscale tracer transport model. *CAS/JSC WGNE Res. Activ. Atmos. Oceanic Modell.*, **39**, 5.29–5.30.

Takakura, T., and T. Komori, 2020: Two-tiered sea surface temperature approach implemented to JMA's Global Ensemble Prediction System. *WGNE. Res. Activ. Earth. Sys. Modell.,* **50**, 6.15-6.16.

Takano, I., Y. Aikawa and S. Gotoh, 2007: Improvement of photochemical oxidant information by applying transport model to oxidant forecast. *CAS/JSC. WGNE. Res. Activ. Atmos. Oceanic Modell.*, **37**, 5.35–5.36.

Tanaka, T. Y. and M. Chiba, 2005: Global simulation of dust aerosol with a chemical transport model, MASINGAR. *J. Meteor. Soc. Japan*, **83A**, 255–278.

Toyoda, T., Y. Fujii, T. Yasuda, N. Usui, T. Iwao, T., Kuragano and M. Kamachi, 2013: Improved analysis of seasonal-interannual fields using a global ocean data assimilation system. *Theoretical and Applied Mechanics Japan*, **61**, 31-48

Verhoef, A., M. Portabella and A. Stoffelen, High-resolution ASCAT scatterometer winds near the coast, IEEE Transactions on Geoscience and Remote Sensing, 2012, 50, 7, 2481-2487

Yoshimura, H. and S. Yukimoto, 2008: Development of a Simple Coupler (Scup) for Earth System Modeling, *Papers in Meteorology and Geophysics*, **59**, 19-29.

Yukimoto, S., H. Yoshimura, M. Hosaka, T. Sakami, H. Tsujino, M. Hirabara, T. Y. Tanaka, M. Deushi, A. Obata, H. Nakano, Y. Adachi, E. Shindo, S. Yabu, T. Ose, and A. Kitoh, 2011: Meteorological Research Institute-Earth System Model Version 1 (MRI-ESM1) - Model Description -,

Technical Reports of the Meteorological Research Institute, **64**, ISSN 0386-4049, Meteorological Research Institute, Japan.

Yukimoto, S., Y. Adachi, M. Hosaka, T. Sakami, H. Yoshimura, M. Hirabara, T. Y. Tanaka, E. Shindo, H. Tsujino, M. Deushi, R. Mizuta, S. Yabu, A. Obata, H. Nakano, T. Koshiro, T. Ose, and A. Kitoh, 2012: A New Global Climate Model of the Meteorological Research Institute: MRI-CGCM3 —Model Description and Basic Performance—. *J. Meteor. Soc. Japan*, **90A**, 23-64, doi:10.2151/jmsj.2012-A02.

Yumimoto, K., H. Murakami, T. Y. Tanaka, T. T. Sekiyama, A. Ogi, and T. Maki, 2016a: Forecasting of Asian dust storm that occurred on May 10–13, 2011, using an ensemble-based data assimilation system, *Particuology*, **28**, 121-130, doi:10.1016/j.partic.2015.09.001.

Yumimoto, K., T. M. Nagao, M. Kikuchi, T. T. Sekiyama, H. Murakami, T. Y. Tanaka, A. Ogi, H. Irie, P. Khatri, H. Okumura, K. Arai, I. Morino, O. Uchino, and T. Maki, 2016b: Aerosol data assimilation using data from Himawari-8, a next-generation geostationary meteorological satellite, *Geophys. Res. Lett.*, **43**, 5886-5894, doi:10.1002/2016GL069298.

Yumimoto, K., T. Y. Tanaka, N. Oshima, and T. Maki, 2017: JRAero: the Japanese Reanalysis for Aerosol v1.0, *Geosci. Model Dev.*, **10**, 3225-3253, doi:10.5194/gmd-10-3225-2017.